Objective 3

Objective 3 Chapter 6

Impacts of the synthesized nanomaterials on soil and plant health

6.1. Introduction

Nanomaterials, including nano-fertilizers and nano-bio-stimulants, offer promising applications at the plant-microbe-soil interface, with enhanced nutrient uptake efficiency and reduced environmental impact[1,2]. Multi-metallic nanoparticles display unique properties and synergistically interact with biological systems, promising improved plant growth, pathogen resistance, and soil fertility[2,3]. Nitrogen-fixing bacteria, such as Rhizobium and Azotobacter, are vital for turning atmospheric nitrogen into an available form for plants, consequently enhancing soil fertility and increasing plant growth[4,5]. Both the Gram-positive and Gram-negative bacteria fared well in antibacterial studies using biosynthesized NPs. Biosynthesized NPs' method of action against bacterial cells is dictated by their eventual bereavement. Positively charged nanoparticles readily bond to negatively charged bacterial cell surfaces, triggering the cell wall to rupture and perish. In hydroponic systems, nano-fertilizers enable precise nutrient uptake and controlled release mechanisms, promoting healthier and more productive crops[2,3]. Unlike traditional soil-based farming, which allows plants to acquire a varied range of nutrients naturally available in the soil, hydroponic systems rely on artificial nutrient solutions, necessitating precise micronutrient monitoring and management[6]. Micronutrient imbalances or shortages can hurt plant growth, resulting in lower yields and poor crop quality. Hydroponic farming offers an overhaul in agricultural operations, replacing traditional soil-based agriculture with rich nutrient solutions for growing plants. This novel strategy has gained great support in recent years, driven by its promise to solve the critical issues of food security and resource shortages. For example, Majid et al. (2021)[7] found that hydroponic systems increased lettuce productivity by 20x when compared to conventional farming approaches. Similarly, Maluin et al. (2023)[8] also observed Chitosan nanoparticles consequently enhancing soil fertility and increasing plant growth[4,5]. Studies have continuously proved soil-less farming's exceptional productivity potential, with researchers finding significant gains in crop yields across numerous plant species[7]. For example, Majid et al. (2021)[7] found that hydroponic systems increased lettuce productivity by 20x when compared to conventional farming approaches. Similarly, Maluin et al. (2023)[8] also observed

Chitosan nanoparticles as a sustainable alternative fertilizer formulation in hydroponically cultivated *Brassica rapa* subsp. chinensis (L.) Hanelt microgreens and mature vegetables. Similarly, Hassanein et al. (2021)[9] harvested lettuce that had 21.0-1,920% higher NP absorption while remaining well below hazardous thresholds.

Chickpea (*Cicer arietinum* L.), a staple legume crop grown in many parts of the world, offers several benefits when grown using traditional soil-based farming methods, especially when supplemented with micronutrient nano fertilizers containing zinc (Zn), copper (Cu), iron (Fe), and manganese (Mn). Chickpeas are noted for their capability to fix nitrogen from the atmosphere via symbiotic partnerships with nitrogen-fixing bacteria, which makes them less reliant on external nitrogen fertilizers than other crops. Chickpea plants can benefit from micronutrient nano fertilizers comprising Zn, Cu, Fe, and Mn, which can help them grow and develop more effectively. These micronutrients serve important roles in a variety of physiological processes, including photosynthesis, enzyme activation, and stress tolerance. Our study emphasized on presenting the effects of novel multimetallic nanomaterials in the microbe-soil-plant interface, their responses to such Zn-based nanoparticles like Zinc Monometallic Nanoparticles (MNP), Zinc Copper Bimetallic Nanoparticles (BNP), and Zinc Copper Iron Manganese Quadrimetallic Nanoparticles (QMNP). In addition, we investigated the physiochemical properties of nano-based metal oxide applications for improving agricultural systems.

6.2. Requisites:

- Stackable Incubator Shaker
- Vertical Autoclave Double Walled
- Petri dishes
- Agar plates
- Microbial strains
- Fixatives
- Antibiotics
- Microplate Spectrophotometer
- Biosafety Cabinet Class II Laminar Air Flow Hood
- Laboratory Centrifuge
- Buffers
- pH meter and EC meter

Chemicals employed in the current investigation were of analytical grade and were bought from Merck, Alfa Aesar, and Hi-Media. All chemical reactions, including the fabrication of leaf extracts, stock solutions, and working solutions, were carried out using ultrapure distilled deionized water (Milli-Q, Millipore Co., Bedford, MA, USA).

6.3. Materials and Methods

6.3.1. Bacterial Compatibility Assay

Bacterial Compatibility assay was done with Agar Well Diffusion Assay (AWDA) involves creating wells in Muller-Hinton agar plates using a sterile cork borer, with test samples added to the wells for diffusion into the agar medium. Zones of inhibition around the wells are then measured to assess antimicrobial activity[10]. MNPs, BNPs and QMNPs synthesized using aqueous leaf extract of *C. lutescens* were evaluated for antibacterial activities against *Salmonella Sp*. and *Rhizobium Sp*. via Agar Well Diffusion Assay (AWDA) technique [11]. Treatments are described in *chapter 3, section 3.4*. Gentamicin served as a positive control, and incubation was conducted at 30 ± 2°C for 24–48 hours to measure diameter of zones of inhibition in millimeter (mm). Next, for SEM study, the bacterial isolates of *Rhizobium sp.,* and *Salmonella typhi* were inoculated onto agar plates with appropriate growth media, and nanoparticles were added as needed. Coverslips sterilized and placed on agar plates allow bacterial growth and interaction with nanoparticles[12]. Following incubation, coverslips are removed and rinsed with buffer solution to eliminate excess media and non-adherent bacteria. Bacterial cells attached to coverslips are then fixed using appropriate fixatives for morphology preservation.

6.3.2. Seed Germination assay and Lab scale Hydroponic farming

Chickpea seeds (*Cicer arietinum* L.) were procured from Krishi Vigyan Kendra in Sonitpur, Assam, India. Germination tests were carried out in sterile petri plates and subsequently transferred to lab-scale hydroponic cultivation for 120 days. Non-nano scale inorganic salts of Zn and Zn-Cu along with Monometallic and Bimetallic Nanoparticle (MNP, BNP) concentrations (50, 100, 200, 250, and 500 mg L^{-1}) were prepared by serial dilution according to Devi et al. (2020)[13], meanwhile for QMNP concentrations were kept low as seeds failed to germinate beyond 50 mg L^{-1}. Thus, both QMNP concentrations and non-nano inorganic salt combinations of Zn, Cu, Fe, and Mn were kept at 5 mg L^{-1}, 15 mg L^{-1}, 25 mg L^{-1}, 40 mg L^{-1}, and 45 mg L^{-1} in a similar manner of serial dilution technique. Treatments are described in *chapter 3, section 3.5*. Seeds were cleansed, disinfected with sodium hypochlorite, and treated with nanoparticle solutions. Incubation was conducted at 22 °C under a 12-hour light cycle for

7 days. The efficacy of the treated samples as plant growth-promoting agents were evaluated based on their effects on plant growth potential concerning Percent Germination, Germination Index (GI), Relative Root Growth% (RRG), and Relative Shoot Growth% (RSG) were assessed with equation (1) (2) (3) (4) after 7 days, revealing an EC_{50} of 500 ppm for nanoparticle-mediated suppression of root length in the case of both MNP and BNP whereas for QMNP it was 45 mg L^{-1} [14–17] (Fig.6.3.)

$$Percent\ germination = \frac{Number\ of\ seeds\ germinated\ in\ treatment}{Total\ number\ of\ seeds\ germinated\ in\ control} \times 100 \quad \text{----------eqn (1)}$$

$$Germination\ Index = (7 \times n1) + (6 \times n2) + (5 \times n3) + (4 \times n4) + (3 \times n5) + (2 \times n6) + (1 \times n7) \text{ ----------eqn (2)}$$

where, n1, n2, n3. . .n7 are several seeds germinated on the first, second, third, and subsequent days until 7th day.

$$RRG(\%) = \frac{Mean\ Root\ length\ of\ treated\ seeds}{\text{Mean Root length of control}} X\ 100 \text{ ----------eqn (3)}$$

$$RSG(\%) = \frac{\text{Mean shoot length of treated seeds}}{\text{Mean shoot length of control}} X\ 100 \text{ ----------eqn (4)}$$

For hydroponic systems, clear wide-mouth plastic containers were taken and net pots were inserted into the mouth of the container. For easy passage of air, four germinated seeds with three replicates per container were kept. No nutrient solutions were used. Base solutions of nanoparticles (MNP, BNP, QMNP) were dissolved in de-ionized water. Control was kept with no amendments. The base solution was changed every 5th day[18,19]. A scale of 30 cm was used to measure the root and shoot length of the plant and a pH meter was used to measure the pH.

6.3.2.1. Total Chlorophyll

Total Chlorophyll content was determined by extracting 100 g of fresh leaf in 10 ml of 80% acetone and measuring absorbance at 645 and 663 nm using a Thermo-Scientific Microplate Spectrophotometer, Multiskan SkyHigh. Total Chlorophyll was calculated using the Anderson and Broadman formula (1966)[20] equation (5). The Chlorophyll stability index was calculated as the ratio of total chlorophyll in the treatment to that in the control, multiplied by 100, following the method outlined by Sairam et al. (1997)[21] Equation (6).

Total Chlorophyll (mg g^{-1}Fresh Weight) = 20.2 (A645) + 8.02(A663) × V1000 × W…….(5)

Where A645 and A663 stand for the extract's absorbance at 645 and 663 nm, respectively. V denotes the weight (g) of the fresh tissue and the volume (mL) of the extract.

$$Chlorophyll\ stability\ index\ (CSI) = \frac{Total\ chlorophyll\ in\ the\ treatment}{Total\ chlorophyll\ in\ control} \times 100 \quad \ldots\ldots\ldots \text{eqn (6)}$$

6.3.2.2 Nutrient uptake

Mineral uptake in hydroponically grown chickpeas was assessed after 120 days of germination, with concentrations reported as weight percentage of fresh plants. 250 mg of fresh plant tissue underwent digestion in HNO_3:$HClO_4$ (9:4) mixture for Atomic Absorption Spectroscopy (AAS) following the protocol of Ma et al. (2001)[22].

6.3.2.3. Biochemical Parameters

6.3.2.3.1. Catalase

Catalase enzyme activity in plants was estimated using the spectrophotometric method[23]. Plant tissue was homogenized in a phosphate buffer and centrifuged to obtain the enzyme extract. The reaction mixture contained hydrogen peroxide (H_2O_2) and enzyme extract, with absorbance changes monitored at 240 nm over time. Enzyme activity was calculated on the basis of the rate of H_2O_2 decomposition, expressed Enzyme activity units mL^{-1} extract. Standard curves with known concentrations of H_2O_2 were used for quantification.

6.3.2.3.2. Peroxidase (POD)

Peroxidase activity in plants was determined spectrophotometrically[24]. Plant samples were homogenized in an extraction buffer and centrifuged to collect the supernatant. The reaction mixture contained substrate and enzyme extract, and absorbance changes were monitored at 470 nm. Enzyme activity was calculated based on the rate of substrate oxidation, typically expressed as Enzyme activity units L^{-1}. Standard curves with known concentrations of the substrate were utilized for quantification.

6.3.2.3.3. Lipid Peroxidation (LPO)

Lipid peroxidation activity in plants was assessed by measuring Thio Barbituric Acid Reactive Substances (TBARS)[25]. Plant tissue was homogenized in a suitable buffer and incubated with TBA reagent at high temperature. After centrifugation, the supernatant absorbance was determined spectrophotometrically at 532nm. The development of pink chromogen represented the level of lipid peroxidation, which was evaluated by comparing standard curves of malondialdehyde equivalents. Lipid peroxidation levels were expressed as micromoles of Malon Di-Aldehyde per gram fresh weight tissue (μ mol MDA g^{-1} FW tissue).

6.3.3. Pot Experiment

Three replicates were employed for each pot experiment using a factorial randomized block design (FRBD). Plastic pot containers with small holes at the bottom were used for proper drainage. Filled about $3/4^{th}$ of the pots with soil and seeds were dug about 1 cm inside the soil.

Base soil was kept for further studies in airtight zipper bags at 4°C. pH, EC and Bulk density of the base soil, control and treatments were recorded before and after experiments. Biochemical assays were performed in between experiments and at harvest. Treatment combinations are described in *chapter 3, section 3.6.* Photosynthesis and stomatal conductance was also recorded for MNP and BNP concentrations (25, 50, 100, 200, 250, 500, 1000 mg kg^{-1}) and QMNP doses (10, 25, 30, 35, 40, and 45 mg kg^{-1}) of nanoparticles, NPK, Vermi-Compost (VC), and Farmyard Manure (FYM) were meticulously mixed with 2.5 kg of soil per pot. The vermicompost was produced in the Soil and Agro Bioengineering Laboratory, at the Department of Environmental Science Tezpur University's where Goswami et al. (2013)[26] established and demonstrated technique for preparing the vermicompost. The feedstock was made up of vegetable waste, crop residue (rice straw and husk), cow dung, and weeds in a 4:2:3:1 ratio and poured into a vermi-bed. *Eisenia fetida,* an earthworm species, was added at a rate of ten worms per kilogram. The mixture was periodically churned and watered to improve aeration and moisture levels. During the incubation period, an ambient temperature of 24-29°C was measured. Both the vermicompost and FYM were obtained from a nearby agrarian farm (Tezpur, Assam) and FYM consisted of 10% rice straw, 15% animal dung slurry, 10% tree leaves, and 65% cow dung. Control pots were maintained without any amendments. soil moisture was checked and added 100 ml of water every 3 days. Each treatment was replicated thrice and contained five seeds were sown per pot. Herein, one plants per pot was designated for morphological, two for biochemical evaluations, and the remainder saved for destructive sampling at harvest at 90 days after sowing (DAS)[27]. After concluding the experiment, the results were analyzed and compared via the analysis of variance (ANOVA).

6.3.3.1. Soil Parameters

6.3.3.1.1. Soil Organic Carbon (SOC)

In this study, soil organic matter was calculated by weighing an oven-dried sample after 6 hours of heating in a muffle furnace at 600° C. Loss on Ignition (LOI) samples were ground and filtered over a 2-nm screen. Samples were taken from the top 0.2 metres of pots[28]. The air-dried materials were ground with a mortar and pestle before being passed through a 150-micrometer sieve. The soil samples were then weighed and placed in a pre-weighed crucible, which was heated in a furnace at approximately 600°C to eliminate organic matter. After cooling, reweigh the crucible to assess the weight loss, which indicates organic matter combustion. Soil organic carbon content is calculated using weight loss and conversion factors and is often reported as a percentage of dry soil weight. Triplicates of each sample were taken, and quality control techniques were assured throughout the analysis's correctness and precision.

6.3.3.1.2. Total Nitrogen (Dumas method)

Samples were prepared by weighing and loading into tin capsules before insertion into the CHNS analyzer (Make: Thermo-Fisher, Model: Flash 2000). The analyser combusts the samples at high temperatures, converting nitrogen compounds into nitrogen gas. The released nitrogen gas is then quantified using thermal conductivity detection. Calibration curves are established using standard nitrogen-containing compounds for accurate measurement. The total nitrogen content in the samples is calculated based on the detected nitrogen gas levels[29]. The process is repeated for multiple samples to ensure accuracy and reproducibility.

6.3.3.1.3. Soil available phosphorous (P)

Bray's reagent[30] was used to extract Soil samples, which helped in releasing the available phosphorus from soil particles. The extracted solution is then filtered to remove particulate matter. Phosphorus concentration in the filtrate is determined spectrophotometrically at specific wavelengths corresponding to phosphate ions. Calibration curves are established using known phosphate standards to quantify the phosphorus concentration in the soil extract[31].

6.3.3.1.4. Available potassium (K)

Available potassium (K) in soils were carefully estimated. Soil samples underwent extraction with ammonium acetate to release available potassium ions, which are then atomized and excited in a flame photometer. Excited potassium ions emit characteristic light at a specific wavelength, measured by a photodetector. Intensity of emitted light correlates with potassium ion concentration, quantified using a calibration curve from known standards. Potassium content is reported as milligrams per kilogram (mg kg^{-1} dry weight soil)[32].

6.3.3.1.5. Photosynthesis rate, stomatal conductance, and transpiration rate

The Li-Cor Li-6400 leaf chamber ensures airtight sealing, controlling CO_2 and light levels while measuring leaf gas exchange parameters. Photosynthetically active radiation (PAR) mimics natural light conditions, while CO_2 concentration is precisely regulated and monitored[33,34]. The Li-6400 calculates the photosynthesis rate based on CO_2 concentration differences, stomatal conductance using water vapor flux, and transpiration rate by measuring water vapor loss from the leaf surface, all about the leaf area.

6.3.3.1.6. Peroxidase (POD)

Referred to the same method described in section 3.2.3.2.

6.3.3.1.7. Estimation of Mineral Content in plant and soil

Estimation of Mineral Content in *Cicer* plants as well as mineral content retention in soils were prepared by digesting the harvested samples after 90 days using suitable acids to solubilize the minerals. The digested samples were diluted to appropriate concentrations for analysis. ICP-

MS was calibrated using standard solutions of known mineral concentrations. The samples were introduced to the instrument's plasma torch, where they were atomized and ionized. calculations were done to report the concentrations in mg kg^{-1} fresh weight tissue[35–37].

6.3.3.1.8. Total Bacterial and Fungal Count

Using the serial dilution approach, bacterial colonies were obtained by plating 100 µl in Petri plates. A colony counter was used to count the colonies that emerged on the plates, and the numbers were reported in terms of Colony Forming Units (CFU g^{-1}). By means of Czapek-Dox and nutrient agar media, a conventional serial dilution technique (10^{-4} dilution) was used to count the total number of colony-forming units for bacteria and fungi, respectively[38,39].

6.4. Results

6.4.1. Bacterial Compatibility Assay

Bacterial Compatibility assay was done to evaluate the Lethal Dose (LD_{50}) of the tailored nanoparticles for their short-term application in chickpea (*Cicer aeritinum* L.) seed germination experiments followed by a hydroponic lab-based study were used to evaluate the effects of monometallic, bimetallic and quadrimetallic nanoparticles on and plant environment. 1000 µg ml^{-1} dose of MNP showed a zone of inhibition, of 0.1±0.03 mm against *Rhizobium sp*.; 1500 µg ml^{-1} of MNP (Table 6.5.) showed an inhibition zone of 0.1±0.02 mm against *Salmonella typhi*. At 2000 µg ml^{-1} MNP showed a distinct clear agar zone with a radius of 0.2±0.06 mm against *Rhizobium sp.,* and a radius of 0.2±0.03 mm was recorded against *Salmonella typhi*. (Fig. 6.8.). Gentamycin was used as positive control, and distinct zones of inhibition at 50 µg mL^{-1} were observed for Gentamycin. At 1000 µg ml^{-1} and 1500 µg ml^{-1} of BNP respectively, the diameter of the zone of inhibition was 0.2±0.02 mm and 0.6±0.1 mm against *Salmonella Typhi* was observed (Table 6.5.). At 2000 µg ml^{-1} BNP showed a zone of inhibition cm against *Rhizobium sp.*, and *Salmonella typhi* radius of 0.1±0.03 mm and 0.8±0.1mm respectively. Lower doses such as 500 µg ml^{-1} of MNP and BNP did not affect the bacterial species, 2000 µg ml^{-1} of MNP and BNP was the most effective anti-bacterial dose, this was confirmed by SEM morphological studies of the MNP-BNP-bacteria interfaces. Although 2000 µg ml^{-1} dose of MNPs and BNPs showed distinct clear zones in agar well, SEM images revealed that the MNPs and BNPs did not have a lethal impact on the *Rhizobium sp.* and *Salmonella typhi* cells. Lower doses such as 500 µg ml^{-1} of QMNP had no effect on the bacterial species (Table 6.6.), however, QMNP at 1500 μg^{-1} ml concentration showed a zone of inhibition of 03.00±0.4 mm against *Rhizobium* sp., and 02.00±0.2 mm against *Salmonella typhi.* At concentration of 2000 µg ml^{-1} of QMNP was the most effective anti-bacterial dose, this was confirmed by SEM morphological studies of the QMNP-bacteria interfaces (Fig. 6.10.).

6.4.2. Seed Germination assay and Lab scale Hydroponic farming

Application of MNPs had an overall positive impact on the Germination Index (GI) of the seeds. The highest germination percentage was documented in 250 mg L^{-1} MNP treated seeds (45%) followed by 200 mg L^{-1} MNP (10%). However, seeds treated with 500 mg L^{-1} MNP showed reduction of 24%. On the other hand, application of non-nanoscale Zn revealed a negative response in GI of the treated seeds. The highest uptake of MNPs was documented at 500 mg L^{-1}, followed by 200 mg L^{-1} in the seedlings. Nutrient uptake estimation was done after 90 days. Overall low Zn uptake was documented with MNPs as compared to its non-nanoscale inorganic Zn salts counterparts; minimum uptake documented at 50 mg kg^{-1} (60% reduction from control) Compared to control MNP-250 mg L^{-1} showed highest Relative Root Growth RRG (%) 117.5 and Relative Shoot Growth RSG (%) 136.3 also the pod yield (g/pod) obtained after 120 days; meanwhile in non-nano scale inorganic salt treatments a decreasing trend in RRG(%), RSG(%) and pod yield (g/pod) was observed (Table 6.1.,6.3.) Moreover, an overall reduction in GI was observed with 100 mg L^{-1} BNP (37% decrease) as compared to control and non-nanoscale Zn-Cu salts. Non-nanoscale Zn-Cu salt showed 59% reduction with 500 mg L^{-1} dose. Non-nanoscale Zn uptake by the test plants was significant with 500 mg L^{-1}, trailed by 250 mg L^{-1}, whereas a low uptake was documented with 50 mg L^{-1}dose. Compared to non-nano scale inorganic salt, a decreasing trend was observed in all treatment groups; BNP-50 mg L^{-1} showed highest RRG (%) 107.5 and RSG (%) 90 also the pod yield (g/pod) of 0.77±0.03 obtained after 120 days. Highest reduction was observed in 500 mg L^{-1} both in BNP treatment and in non-nano scale inorganic Zn-Cu salt. (Table 6.1., 6.3.). Conversely, low uptake of zinc was observed in BNP treated seeds in the concentration of 50 mg L^{-1} and non-nano scale zinc 50 mg L^{-1}. Nevertheless, uptake of Copper in BNP treated seeds was significantly higher in 500 mg L^{-1} followed by 250 mg L^{-1}. A similar trend was also delineated in non-nano scale copper with the highest increase in 500 mg L^{-1} trailed by 250 mg L^{-1}. Application of QMNPs had an overall positive impact on the Germination Index (GI) and % germination of the seeds with highest GI and % germination noted in 5 mg L^{-1} QMNP. However, lowest GI and % germination was documented under Non nanoscale QM application at the rate of 45 mg L^{-1}. Amongst the nanoparticle treated seedlings, highest uptake of Zinc and Copper was documented in 45 mg L^{-1} treatment and iron uptake highest was documented in 40 mg L^{-1} and Manganese uptake was highest in 45 mg L^{-1}, similar trend was also noted in non-nano-scale treatments. (Table 6.3.). Compared to control, an overall decreasing trend was observed in QNP treated seeds with an exception in QNP-25 mg L^{-1} showed highest Relative Root Growth RRG (%) 107.8 and Relative Shoot Growth RSG (%) 119.7 also the pod yield (g/pod) of 1.90±0.04

obtained after 120 days; meanwhile in non-nano scale inorganic salt treatments a steady decrease in RRG(%), RSG(%) and pod yield (g/pod) was observed.

Table 6.1. Germination profile, RRG (%), and RSG (%) profiling of *Cicer arietinum* (L.) seedlings exposed to various doses of MNP and BNP for a period of 7 Days.

Treatments	G. I	Germination %	RRG (%)	RSG (%)
Control	25.7±4.04	76.7±5.77	100.0	100.0
MNP-C1	24.7±1.15	73.3±5.77	108.3	93.4
MNP-C2	27.7±0.58	86.7±5.77	107.8	102.5
MNP-C3	28.3±1.15	86.7±5.77	75.0	116.1
MNP-C4	37.3±8.08	96.7±5.77	117.5	136.3
MNP-C5	19.3±2.31	63.3±5.77	92.2	84.7
Nn-Zn(C1)	7.7±2.08	23.3±5.77	88.5	75.7
Nn-Zn(C2)	12.3±2.08	36.7±5.77	79.3	75.9
Nn-Zn(C3)	25.7±1.53	73.3±11.55	54.6	76.2
Nn-Zn(C4)	10.0±1.00	26.7±5.77	84.8	76.8
Nn-Zn(C5)	7.7±2.08	23.3±5.77	76.4	65.0
LSD (p≤ 0.05)	**2.538**	**5.318**	**N/A**	**N/A**
Control	25.7±4.04	46.7±5.77	100.0	100.0
BNP-C1	21.0±3.00	53.3±11.55	107.5	90.0
BNP-C2	16.0±1.73	23.3±5.77	106.3	96.2
BNP-C3	25.0±1.00	66.7±5.77	102.6	101.3
BNP-C4	25.7±2.52	66.7±5.77	105.2	121.3
BNP-C5	23.7±1.53	50.0±10.00	79.9	90.1
Nn-ZnCu(C1)	14.7±1.53	46.7±5.77	80.7	65.0
Nn-ZnCu(C2)	13.0±1.73	43.3±5.77	77.0	72.4
Nn-ZnCu(C3)	18.0±2.65	56.7±5.77	81.6	67.8
Nn-ZnCu(C4)	17.0±4.58	43.3±5.77	75.3	71.6
Nn-ZnCu(C5)	10.3±1.53	33.3±5.77	64.4	65.5
LSD (p≤ 0.05)	**2.113**	**5.685**	**N/A**	**N/A**

Table 6.2. Germination profile, RRG (%), and RSG (%) profiling of *Cicer arietinum* (L.) seedlings exposed to various doses of QMNP for a period of 7 Days.

Treatments	GI	Germination(%)	RRG (%)	RSG(%)
Control	25.67±4.04	46.67±5.77	100.0	100.0
QNP-C1	29.67±2.31	93.33±11.55	90.5	94.4
QNP-C2	27.00±4.36	83.33±11.55	99.4	99.8
QNP-C3	25.00±3.46	76.67±5.77	107.8	119.7
QNP-C4	24.67±2.52	76.67±5.77	67.8	90.5
QNP-C5	19.67±1.15	56.67±5.77	63.8	86.4
Nn-QMC1	25.00±1.73	76.67±5.77	64.4	65.7
Nn-QMC2	21.00±1.73	66.67±5.77	64.4	65.7
Nn-QMC3	29.00±1.00	83.33±11.55	64.4	62.6
Nn-QMC4	24.00±4.36	76.67±11.55	56.6	61.1
Nn-QMC5	15.00±5.57	33.33±5.77	52.3	59.9
LSD	**2.6660**	**6.8160**		

Table 6.3. Yield(g/pod) and Micronutrient uptake profiling of *Cicer arietinum* (L.) seedlings exposed to various doses of MNP and BNP for a period of 120 days in a hydroponic growth environment.

Treatments	**Yield (g/pod)** (Mean±SD)	**Zn Uptake (mg Zn kg^{-1} FW tissue)** (Mean±SD)	**Cu Uptake mg Cu kg^{-1} FW tissue**
Control	0.60±0.01	346.0±3.61	
MNP-C1	1.04±0.02	555.7±2.02	
MNP-C2	1.06±0.02	872.3±2.02	**N/A**
MNP-C3	1.07±0.01	1245.0±1.80	
MNP-C4	1.15±0.03	938.8±5.01	
MNP-C5	0.51±0.01	1346.8±2.52	
Nn-Zn(C1)	0.98±0.04	1139.0±1.50	
Nn-Zn(C2)	0.68±0.03	1272.8±1.76	
Nn-Zn(C3)	0.75±0.04	1482.2±1.26	
Nn-Zn(C4)	0.53±0.02	1465.5±8.89	
Nn-Zn(C5)	0.40±0.03	1490.5±1.50	
LSD (p≤ 0.05)	**0.19**	**2.954**	
Control	0.60±0.01	346.0±3.61	154.33±8.69
BNP-C1	0.77±0.03	1068.3±8.74	1005.17±3.55
BNP-C2	1.25±0.03	1133.3±11.34	1042.67±4.86
BNP-C3	1.54±0.04	1309.7±7.69	1305.17±4.25
BNP-C4	1.58±0.03	1345.2±2.75	1291.67±5.01
BNP-C5	0.47±0.03	1484.8±9.78	1458.17±48.97
Nn-ZnCu(C1)	0.84±0.04	1071.0±12.82	921.67±10.52
Nn-ZnCu(C2)	1.17±0.04	1160.5±16.12	1072.33±4.65
Nn-ZnCu(C3)	0.96±0.04	1269.0±20.43	1167.50±7.37
Nn-ZnCu(C4)	0.53±0.02	1282.8±12.86	1203.00±33.22
Nn-ZnCu(C5)	0.38±0.03	1320.3±8.33	1269.83±14.78
LSD (p≤ 0.05)	**0.24**	**9.394**	**15.688**

Table 6.4. Yield(g/pod) and Micronutrient uptake profiling of *Cicer arietinum* (L.) seedlings exposed to various doses of QMNP for a period of 120 days in a hydroponic growth environment.

Treatments	**Yield (g/pod)** (Mean±SD)	**Zn Uptake (mg Zn kg^{-1} FW tissue)** (Mean±SD)	**Cu Uptake (mg Zn kg^{-1} FW tissue)** (Mean±SD)	**Fe Uptake (mg Zn kg^{-1} FW tissue)** (Mean±SD)	**Mn Uptake (mg Zn kg^{-1} FW tissue)** (Mean±SD)
Control	0.60±0.01	346.0±3.6	154.3±8.7	176.8±13.7	72.7±10.8
QMNP-C1	1.05±0.05	782.3±21.0	638.3±38.7	724.2±5.3	687.0±4.8
QMNP-C2	1.27±0.03	923.3±10.5	720.8±7.8	727.3±7.3	667.0±21.4
QMNP-C3	1.90±0.04	921.7±7.4	767.5±12.7	826.7±17.8	686.0±87.9
QMNP-C4	0.74±0.04	978.2±13.9	914.3±5.8	1024.0±47.0	924.7±11.5
QMNP-C5	0.40±0.02	1024.0±11.3	989.3±9.9	1004.8±24.8	1019.7±12.2
Nn-QMC1	0.94±0.03	738.8±19.7	649.3±9.7	711.7±4.4	678.7±2.5
Nn-QMC2	1.07±0.03	717.0±14.9	681.7±8.6	661.8±4.4	633.8±7.3
Nn-QMC3	0.78±0.04	921.5±9.1	842.5±4.8	810.0±2.6	784.8±17.6
Nn-QMC4	0.48±0.03	1062.2±13.3	1022.8±14.5	1014.2±3.0	989.2±4.5
Nn-QMC5	0.32±0.01	1116.7±8.5	1035.5±22.5	1020.5±9.7	1016.2±15.4
LSD	**0.03**	**10.58**	**13.11**	**14.687**	**23.662**

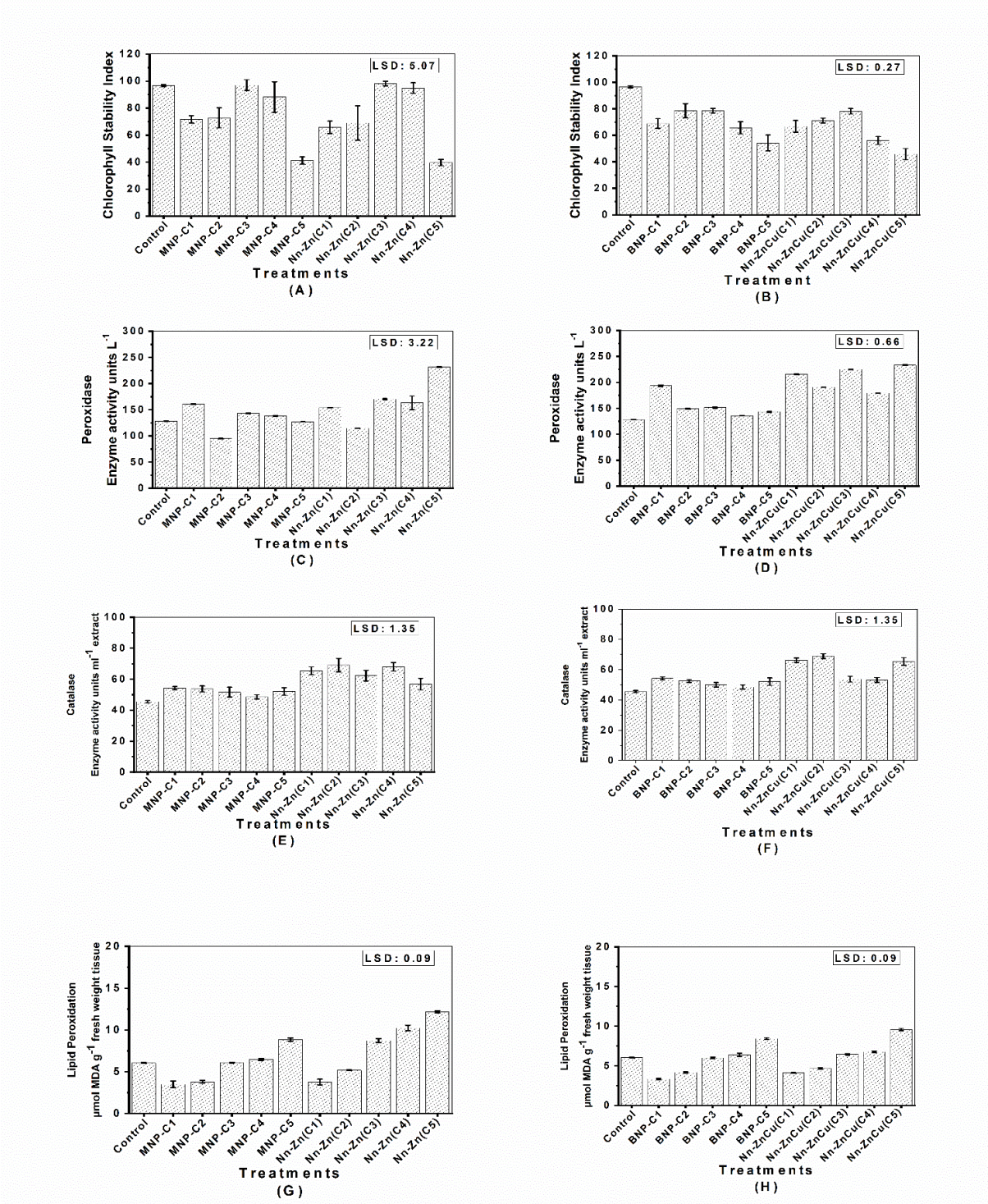

Fig. 6.1. Chlorophyll Stability Index (CSI) of MNP and BNP treated seedlings (A-B) after 30 Days. Peroxidase activity of the seedlings as affected by the application of MNP and BNP (C-D), Catalase activity of the seedlings (E-F), and LPO content of the seedlings as affected by the application of (G-H).

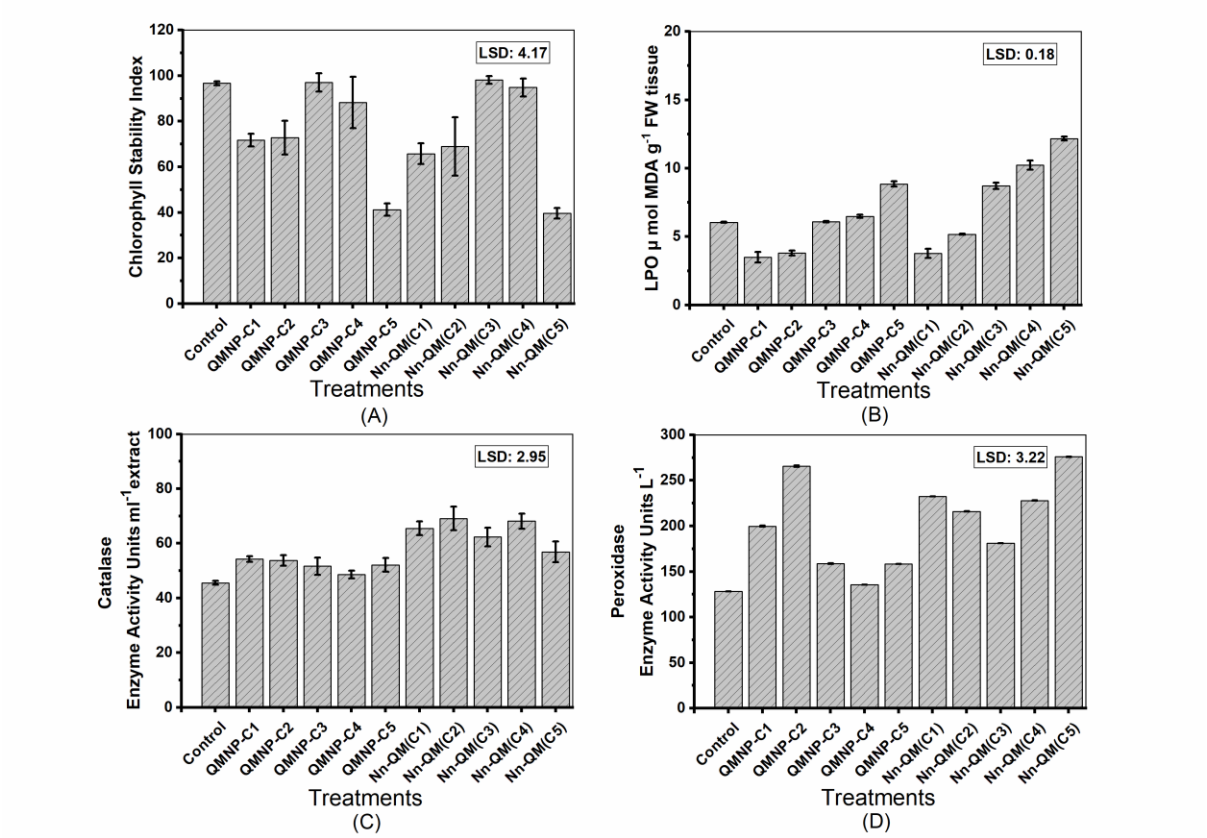

Fig. 6.2. Chlorophyll Stability Index (A). LPO content (B), Catalase activity (C), and Peroxidase activity (D) of the seedlings as affected by the application of QMNP after 30 Days

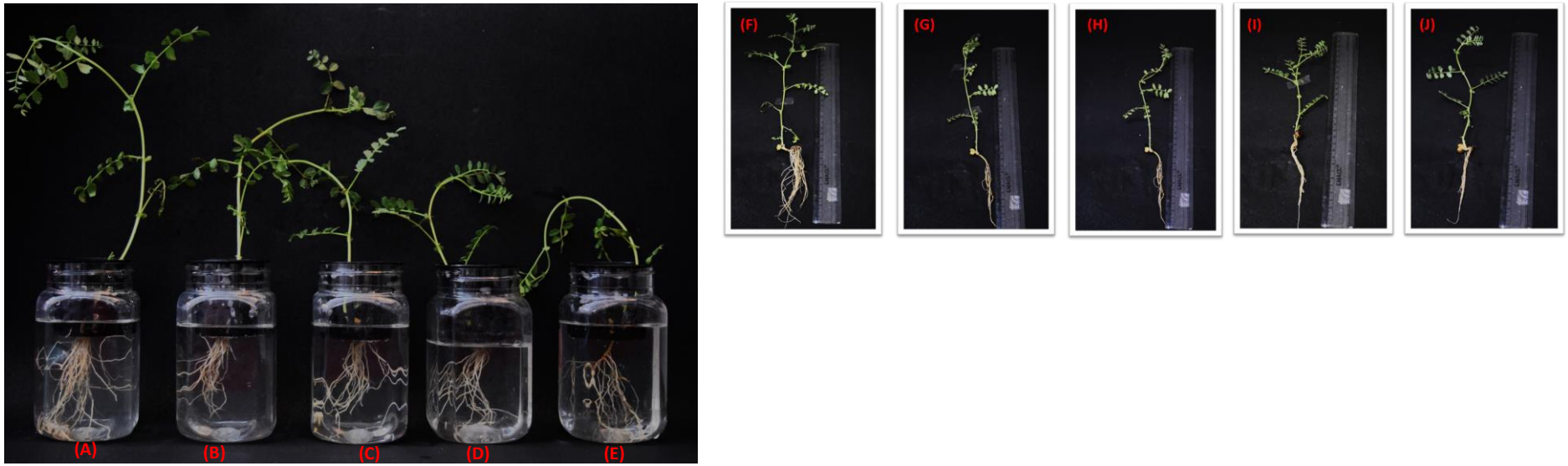

Fig. 6.3. Hydroponically grown *Cicer arietinum* L. where (A) represents MNP-C1, (B) represents MNP-C4, (C) represents BNP-C1, (D) represents BNP-C4 and (E) represents Control. Root length and Shoot length measurement was taken at vegetative stage of *Cicer arietinum* lifecycle (F) MNP-C1, (G) MNP-C4, (H) BNP-C1, (I) BNP-C4.

6.4.2.1. Total Chlorophyll

Total Chlorophyll was estimated with eqn (5) and then the Chlorophyll Stability Index (CSI) was done with eqn (6) at vegetative stage i.e., 30 DAS; notable with 200 mg L^{-1}, trailed by 250 mg L^{-1} doses of MNPs in the seedlings, whereas 50 mg L^{-1} and 100 mg L^{-1} doses of MNPs delineated a low stability under the same experimental conditions. However, chlorophyll stability was high at 500 mg L^{-1} of MNPs. Chlorophyll Stability Index (CSI) varied with MNP and BNP treatments, with optimal stability at specific concentrations[40]. Overall, low stability was observed with application of 200 mg L^{-1} of non-nanoscale Zn (Fig. 6.1.). The CSI was significantly high in BNP treated seeds, with doses of 500 mg L^{-1} whereas it was quite low with 100 mg L^{-1} and 200 mg L^{-1} doses. An overall increase in CSI was found in non-nanoscale Zn-Cu at 500 mg L^{-1} followed by 250 mg L^{-1} (Fig. 6.1.). The Chlorophyll Stability Index (CSI) was notable with 25 mg L^{-1}, trailed by 40 mg L^{-1} doses of QMNPs in the seedlings, whereas 45 mg L^{-1} and 5 mg L^{-1} doses of QMNPs showed a low stability under the same experimental conditions. An overall increase in CSI was found in non-nanoscale QM inorganic salt at higher concentrations (Fig. 6.2.). MNPs were reported to enhance seedling growth and the production of essential nutrients and antioxidant enzymes in plants[41].

6.4.2.2 Nutrient uptake

Non-nanoscale Zn uptake by the test plants was significant with 500 mg L^{-1}, trailed by 250 mg L^{-1}, whereas a low uptake was documented with 50 mg L^{-1}dose. Overall low Zn uptake was documented with MNPs as compared to its non-nanoscale inorganic Zn salts counterparts; minimum uptake documented at 50 mg kg^{-1} (60% reduction from control). The highest uptake of MNPs was logged at 500 mg L^{-1}, followed by 200 mg L^{-1} in the seedlings (Table 6.3.). Conversely, low uptake of zinc was observed in BNP treated seeds in the treatment of 50 mg L^{-1} and non-nano scale zinc 50 mg L^{-1}. Nevertheless, uptake of Copper in BNP treated seeds was significantly higher in 500 mg L^{-1} followed by 250 mg L^{-1}. A similar pattern was also observed in non-nano scale copper with the highest increase in 500 mg L^{-1} followed by 250 mg L^{-1} (Table 6.3.). Amongst the QMNP treated seedlings, highest uptake of Zinc and Copper was observed in 45 mg L^{-1} treatment and iron uptake highest was observed in 40 mg L^{-1} and Manganese uptake was highest in 45 mg L^{-1}, similar trend was noted in non-nano-scale treatments (Table 6.4.)

6.4.2.3. Biochemical Parameters

6.4.2.3.1. Catalase

Oxidative stress enzymes showed marked responses to MNP, BNP and non-nanoscale Zn-Cu treatments. A significantly lower catalase activity was documented in MNP treated seedlings as compared to non-nanoscale Zn treatments. MNP treated seedlings showed a comparatively lower catalase activity with the lowest activity recorded under 200 mg L^{-1} MNP, trailed by 500 mg L^{-1} subsequently. Lower catalase activity was recorded with application of 200 mg L^{-1} and 500 mg L^{-1} Zn salt (Fig.6.1.). Meanwhile, in BNP treated seedlings a higher catalase activity was witnessed in 50 mg L^{-1} and lowest in 250 mg L^{-1} (Fig.6.1.). Catalase activity showed an overall increase in non-nanoscale QM salt applied seedlings as compared to QMNP treated seedlings, regardless of application dose (Fig.6.2.).

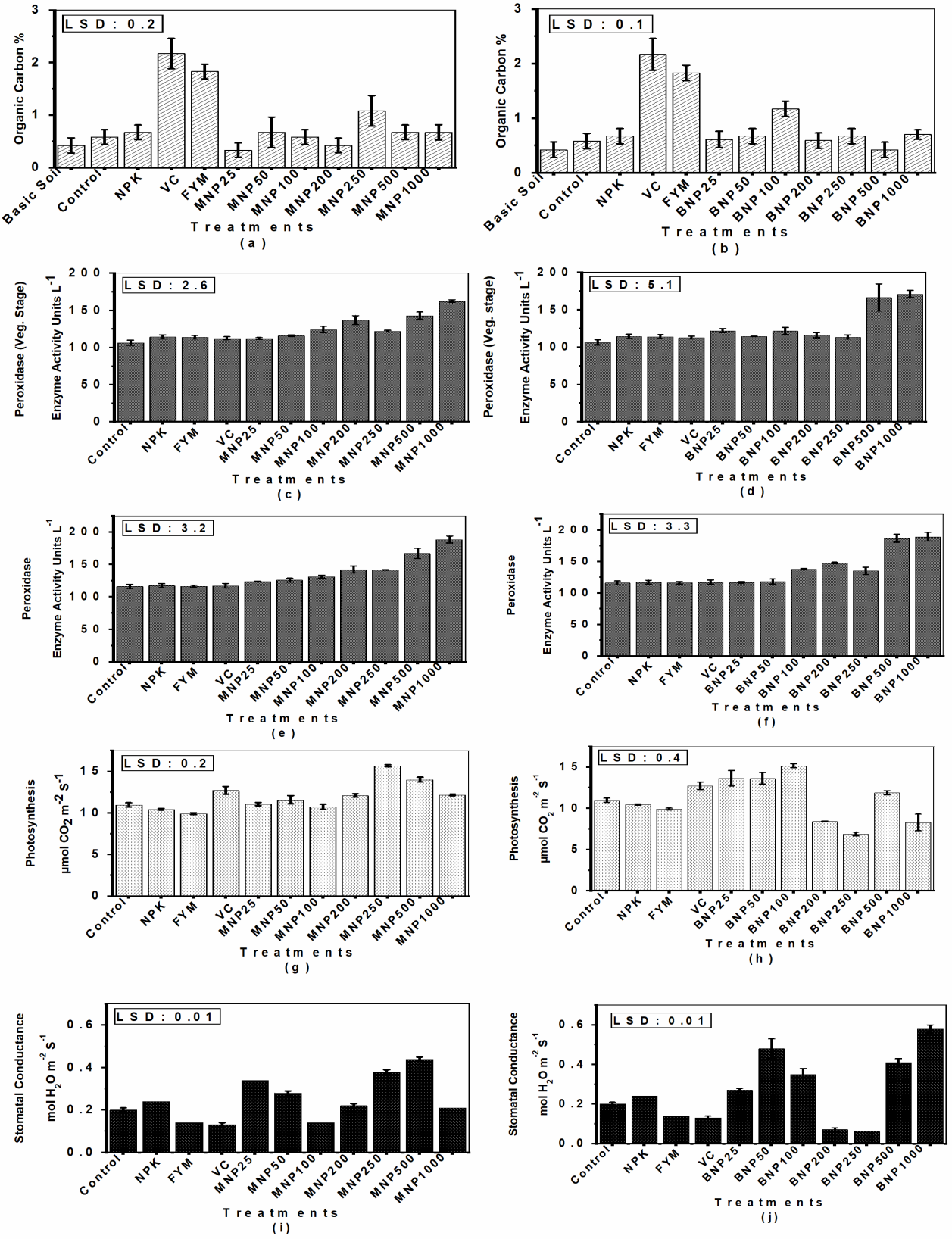

Fig. 6.4. Soil organic Carbon (a-b), Peroxidase at vegetative stage (c-d), Peroxidase at reproductive stage (e-f), photosynthesis (g-h), and stomatal conductance (i-j) of *Cicer arietinum* crops grown in soil under the application MNP and BNP.

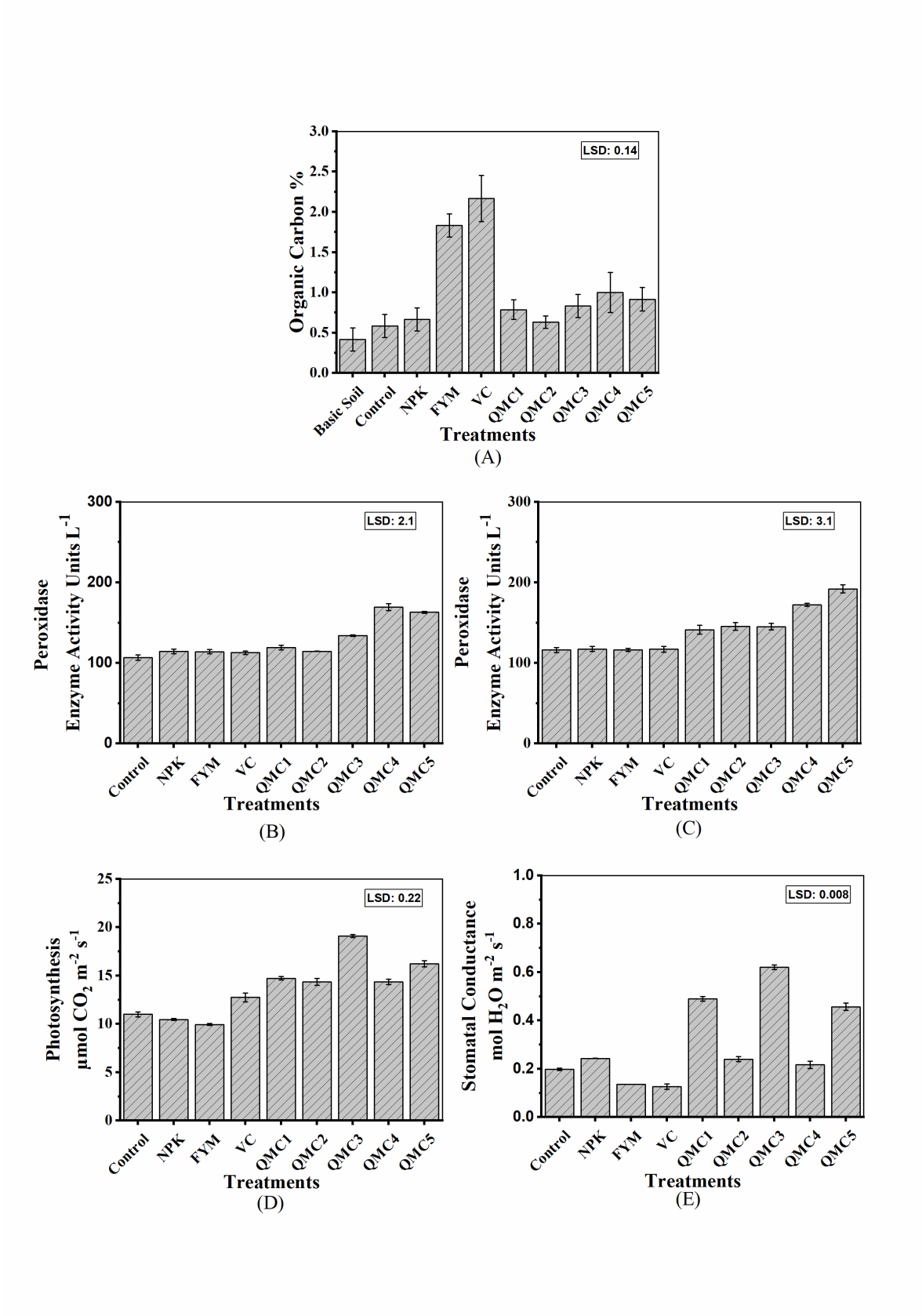

Fig. 6.5. Soil organic Carbon (A), Peroxidase at vegetative stage (B), Peroxidase at reproductive stage (C), photosynthesis (D), and stomatal conductance (E) of *Cicer arietinum* crops grown in soil under the application QMNP

6.4.2.3.2. Peroxidase

The POD activity of seedlings was significantly lower with 100 mg L^{-1} MNPs dose, while moderately higher with 50 mg L^{-1} MNPs treatment than control. The POD activity at 250 and 500 mg L^{-1} non-nanoscale Zn treatment showed highest POD activity (27% and 80% respectively) (Fig. 6.1). Contrastingly, higher peroxidase activity was observed in BNP-C1 (Zinc Copper Bimetallic nanoparticles @ 50 mg L^{-1}), however, compared to control BNP-C4 (Zinc Copper Bimetallic nanoparticles @ 250 mg L^{-1}) showed relatively lower POD level. Moreover, in the case of non-nano scale inorganic salts, an increasing trend of POD activity was observed except in Nn-ZnCu(C2) i.e., 100 mg L^{-1} compared to control (Fig.6.1.). Similarly, Peroxidase activity was noted to be higher in non-nanoscale QM salt application, especially at higher doses (Fig. 6.2.).

6.4.2.3.3. Lipid Peroxidation (LPO)

A similar trend was documented in non-nano scale zinc copper treated seedlings. A conspicuous reduction in LPO activity was observed with MNPs treatment, maximum reduction with 50 mg L^{-1} concentration, followed by 100 mg L^{-1} (Fig. 6.1). Compared to control, an increasing trend of LPO activity was observed in all treatment groups of BNP, with highest activity in 500 mg L^{-1}. A comparable trend was also noted in non-nano scale Zn-Cu inorganic salt treatment groups (Fig. 6.1). A noticeable reduction in LPO activity was observed with QMNPs treatment with maximum reduction at 5 mg L^{-1} concentration, followed by 15 mg L^{-1}, except at higher doses. On the other hand, application of non-nano scale zinc salt also showed a decline in LPO activity with prominent reduction at 5 mg L^{-1} followed by 15 mg L^{-1}. However, an increase in LPO activity was noted when the non-nanoscale QM salt was applied at the rate of 40 mg L^{-1} (Fig.6.2.)

6.4.3. Soil based Study

6.4.3.1. Soil Parameters

6.4.3.1.1. Soil Organic Carbon (SOC)

Soil Organic carbon at harvest was documented to be significantly higher in vermicompost (VC) and FYM treated soils. Furthermore, it was documented to be higher in soils treated with MNP, irrespective of the application rates, especially under 250 mg kg^{-1} MNP (Fig. 6.4). Significantly higher soil organic carbon was documented in BNP treated soil, with highest value documented at 100 mg kg^{-1} (Fig. 6.4). Soil organic C delineated a significant enhancement over control at harvest with highest retention by 45 mg kg^{-1} QMNP treated soils (Fig. 6.5).

6.4.3.1.2. Total Nitrogen

At harvest, MNP treated soils delineated a lower N retention, especially under 200 and 500 mg kg^{-1} treatments. However, higher N retention was noted in 50 mg kg^{-1} MNP treated soils (Table 6.8.). Lowest N retention at harvest was documented in plants treated with 25 mg kg^{-1} BNP, followed by 250 mg kg^{-1} BNP (Table 6.10.). However, rest of the treatments delineated a higher N content at harvest (Table 6.8.). Compared to control, an overall increased Available N retention in soil was documented across the QMNP treatments at harvest (Table 6.12.).

6.4.3.1.3. Soil available phosphorous (P)

Lower P retention in soil was documented in 250 mg kg^{-1} treatment in case of MNP treatment (Table 6.8.). An overall reduction in P retention in soil was documented under BNP application with notable reduction observed at 25 mg kg^{-1}. However, an increased P retention was noted in 200 followed by 250 mg kg^{-1} (Table 6.10.). Compared to control, an overall increased Available P retention in soil was documented across the QMNP treatments at harvest (Table 6.12.).

6.4.3.1.4. Available potassium (K)

Estimation of available potassium (K) in plants as well as in soils were carefully estimated. High K uptake was noted in 500 mg kg^{-1} followed by 250 mg kg^{-1} in MNP treated plants. Moreover, Lower K retention was documented in the MNP treated soils, especially under 50 mg kg^{-1} MNP treatment (Table 6.8.). Contrastingly, an overall increase in K retention in soil at harvest was documented under BNP application with notable increase at 250 mg kg^{-1}. However, a decrease of the same was noted under 200 and 500 mg kg^{-1} (Table 6.10). Contrastingly, an overall lower Available K was revealed by the QMNP treated soils (Table 6.12.)

6.4.3.1.5. Photosynthesis rate, stomatal conductance, and transpiration rate

Compared to control, an overall higher photosynthesis and stomatal conductance was noted in plants especially those treated with 250 mg kg^{-1} MNP (Fig.6.4.) Significantly higher photosynthesis and stomatal conductance was noted at lower doses of BNP application viz. 25, 50, and 100 mg kg^{-1} (Fig. 6.4) Significantly higher photosynthesis and stomatal conductance was delineated by the QMNP treated plants across the treatments with higher values recorded for 10, 35 and 45 mg kg^{-1} (Fig.6.5.)

6.4.3.1.6. Peroxidase (POD)

MNP-treated plants exhibit lower peroxidase activity during the vegetative stage, possibly due to MNP-induced stress alleviation. However, higher peroxidase activity at reproductive stages with higher MNP doses indicates a hormetic response, where moderate stressors induce beneficial physiological responses. Irrespective of the stages of growth, and nanoparticle type, significantly higher peroxidase activity was documented in 500 and 1000 mg kg^{-1} treatments

with an exception in QMNP treated plants where highest peroxidase activity was documented in 40 and 45 mg kg^{-1} treatments.

6.4.3.1.7. Estimation of Mineral Content in plant and soil

Estimation of Mineral Content in plants as well as mineral content retention in soils were carefully estimated. Significantly lower Fe uptake was noted in MNP treated plants with lowest uptake noted under 25 mg kg^{-1} followed by 100 mg kg^{-1} dose. Higher Zn uptake was documented in 1000 mg kg^{-1} MNP application, followed by 250 mg kg^{-1} application. Similarly, higher Cu uptake was documented in 25 mg kg^{-1} MNP application. However, a reduction of the same was noted in rest of the treated plants. Significantly higher Mn uptake was documented in 50, 100, and 200 mg kg^{-1} MNP treated plants (Table 6.7). Application of BNP resulted in a declined Fe uptake in plants, especially at lower doses. Whereas enhanced K uptake was noted in the same, with highest uptake noted under 250, followed by 500 mg kg^{-1}. Highest Zn uptake was documented in 1000 mg kg^{-1} BNP treatments, followed by 200 and 250 mg kg^{-1} treated plants. Furthermore, highest Cu uptake was noted in BNP treated plants irrespective of the application rate, with highest uptake noted under 250, followed by 200 mg kg^{-1} BNP. An overall higher Mn uptake was documented in BNP-treated plants with the highest uptake documented under 1000, followed by 250 mg kg^{-1} BNP application (Table 6.9). At harvest, nutrient uptake viz. Fe, K, Zn, Cu, and Mn, revealed a positive response in their accumulation. Uptake of minerals by *Cicer* plants were quite in trend with higher accrual rates were correlated to higher application doses viz. 35, 40, and 45 mg kg^{-1} across the minerals in QMNP treatment groups compared to control (Table 6.11.).

Significantly higher Fe retention was observed in MNP treated soils, especially under 200, followed by 250 mg kg^{-1} MNP-treated soils and lower retention was observed in 50 mg kg^{-1}. Zn retention in soil was significantly lower under lower doses viz. 25, 50, and 100 mg kg^{-1}. However, Zn retention was significantly higher under higher doses, viz. 250, 500 and 1000 mg kg^{-1} treatments. Irrespective of the treatments, Cu retention delineated to be significantly lesser in MNP-treated soils, especially under 25, followed by 250 mg kg^{-1}. As compared to the control, Mn uptake was noted to be at par under MNP-treated soils (Table 6.7). At harvest, in BNP treatments, an overall decreasing trend was observed for Fe retention with a significant reduction noted for 200 mg kg^{-1}. However, an exception was noted for 25, 50, 500 mg kg^{-1}. Regardless of the application doses, an increase in Zn, Cu and Mn retention was noted across BNP applied soils with the highest retention noted for 500 and 1000 mg kg^{-1} (Table 6.9.). Contrastingly, an overall lower retention of Zn, Cu was revealed by the QMNP-treated soils.

Compared to control, an overall increased Fe, Mn retention in soil was documented across the QMNP treatments at harvest (Table 6.11.).

Table 6.5. Antibacterial activity of biosynthesized MNP and BNP against Pathogenic soil bacteria (*Salmonella typhi*) and non-pathogenic soil bacteria (*Rhizobium*) for evaluation of zone of inhibition with the help of Agar Well Diffusion Assay (AWDA).

	Diameter of inhibition zone in mm (Mean±SD)	
Concentration of material	**Non-pathogenic soil bacteria (*Rhizobium*)**	**Pathogenic soil bacteria (*Salmonella*)**
MNP 500µg^{-1} ml	-	-
MNP 1000µg^{-1} ml	0.1±0.03	-
MNP 1500µg^{-1} ml	0.2±0.04	0.1±0.02
MNP 2000µg^{-1} ml	0.2±0.06	0.2±0.03
BNP 500µg^{-1} ml	-	-
BNP 1000µg^{-1} ml	-	0.2±0.02
BNP 1500µg^{-1} ml	-	0.6±0.1
BNP 2000µg^{-1} ml	0.1±0.03	0.8±0.1

Table 6.6. Antibacterial activity of biosynthesized QMNP against Pathogenic soil bacteria (*Salmonella typhi*) and non-pathogenic soil bacteria (*Rhizobium*) for evaluation of zone of inhibition with the help of Agar Well Diffusion Assay (AWDA).

	Diameter of zone of inhibition in mm (Mean±SD)	
Concentration of material	**Non-pathogenic soil bacteria (*Rhizobium sp.,*)**	**Pathogenic soil bacteria (*Salmonella typhi*)**
QMNP 500µg^{-1} ml	-	-
QMNP 1000µg^{-1} ml	0.2±0.03	-
QMNP 1500µg^{-1} ml	0.3±0.04	0.2±0.02
QMNP 2000µg^{-1} ml	0.4±0.06	0.3±0.03

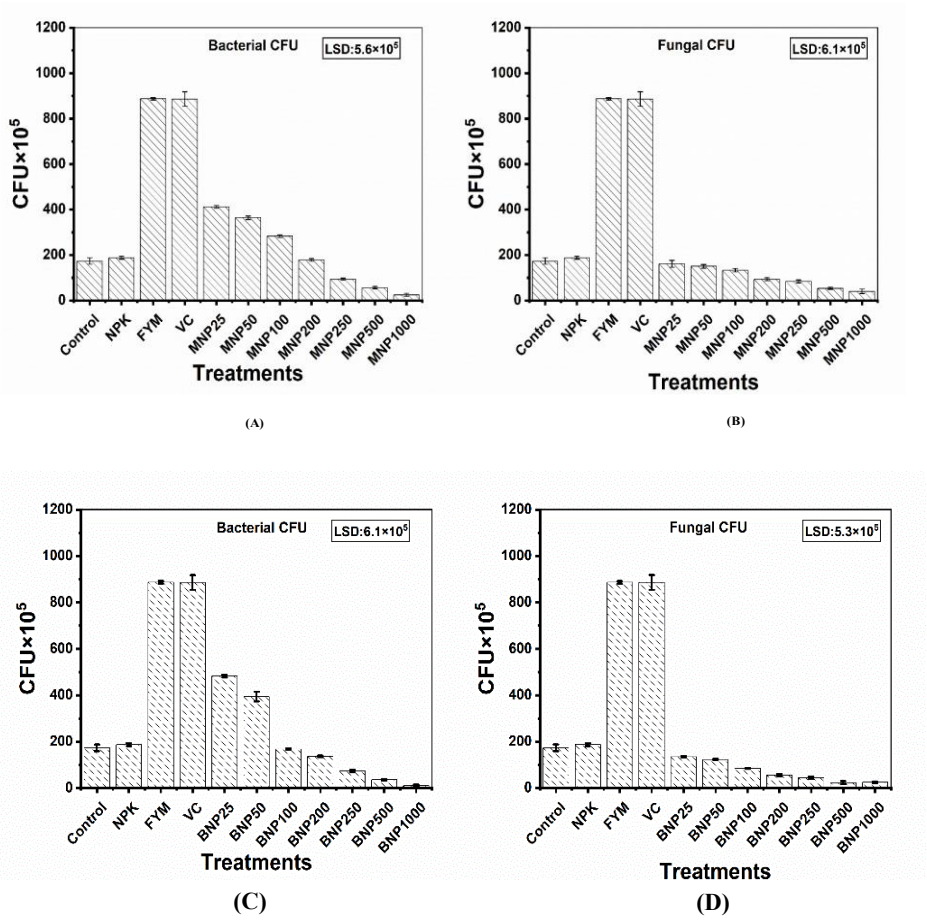

Fig. 6.6. Bacterial and fungal CFU as affected by the application of MNP and BNP in *Cicer arietinum* at harvest

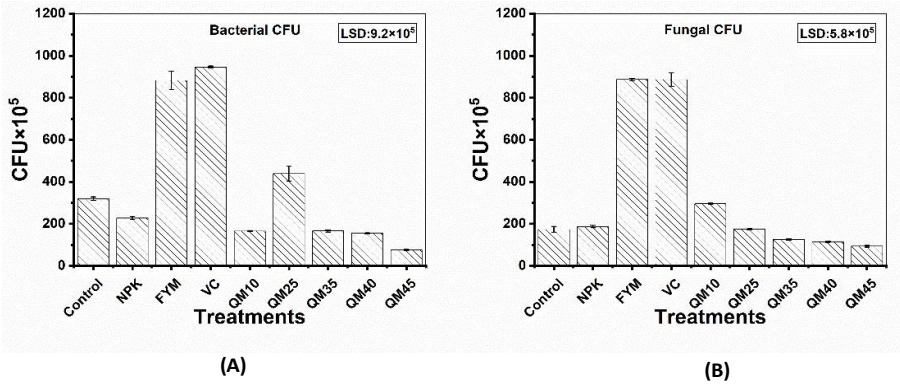

Fig. 6.7. Bacterial and fungal CFU as affected by the application of QMNP in *Cicer arietinum* at harvest

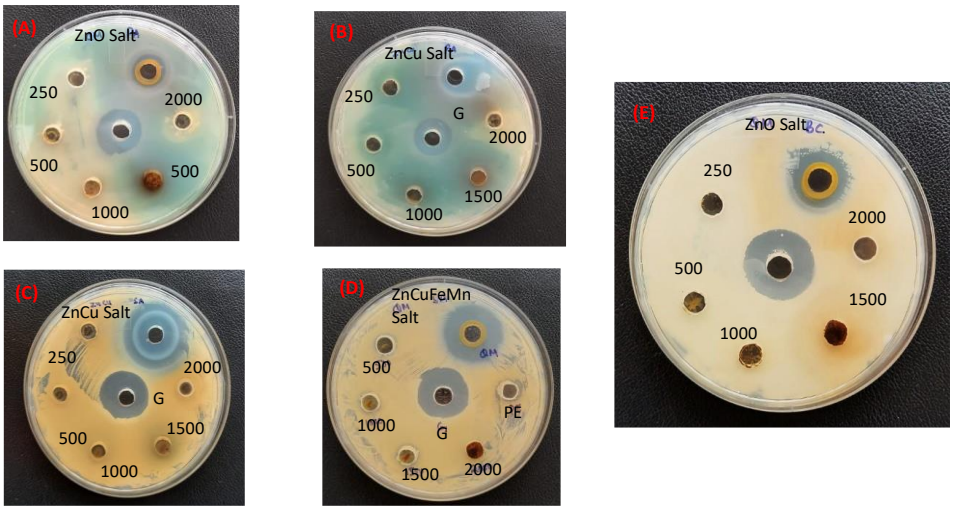

Fig. 6.8. Biocompatibility activity of MNP, BNP and QMNP produced with leaf extract against soil microbial strains (a) *Salmonella typhi*., (d) *Rhizobium Sp*., Numbers denotes concentration in µg ml^{-1}

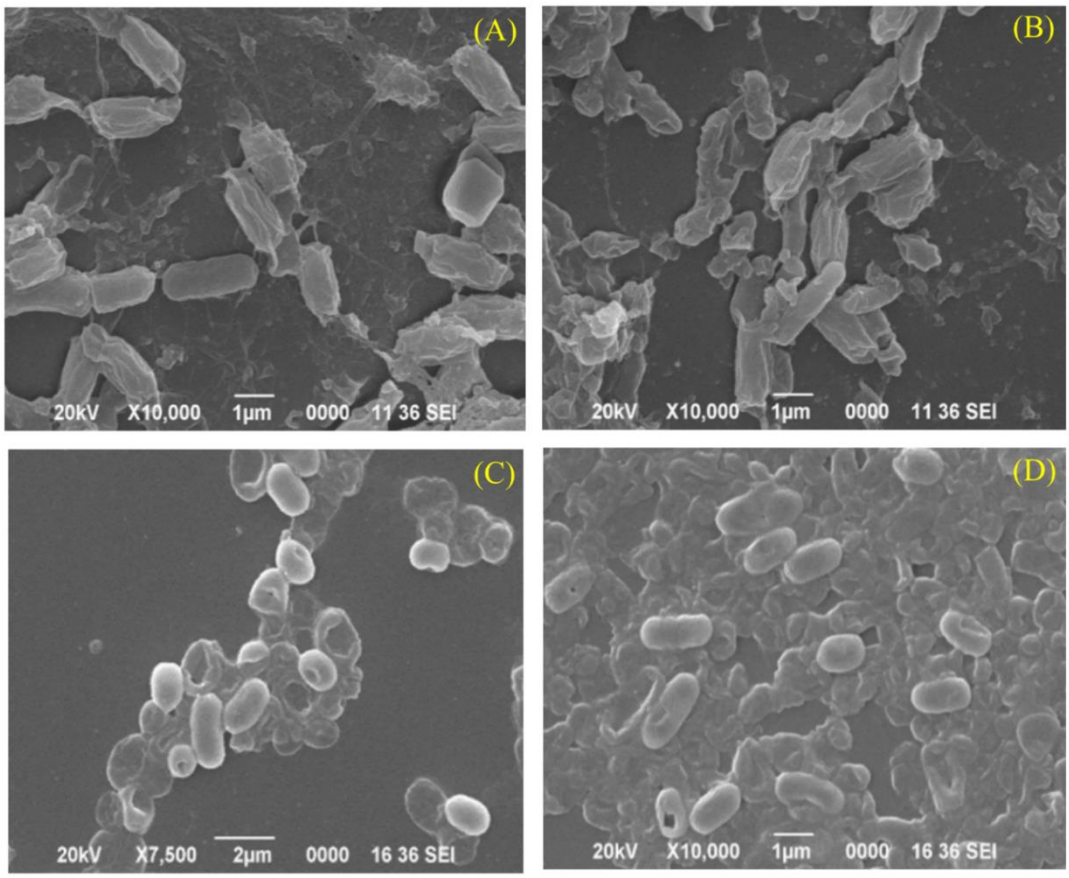

Fig. 6.9. SEM Morphological study micrographs of Biocompatibility activity study of MNP-BNP against soil microbial strains (a) *Rhizobium Sp*., (b) *Salmonella Sp*., (c) *Bacillus Sp*., (d) *Pseudomonas Sp*., and (e) *Staphylococcus aureus*., Note : Numbers denotes concentration in µg/ml

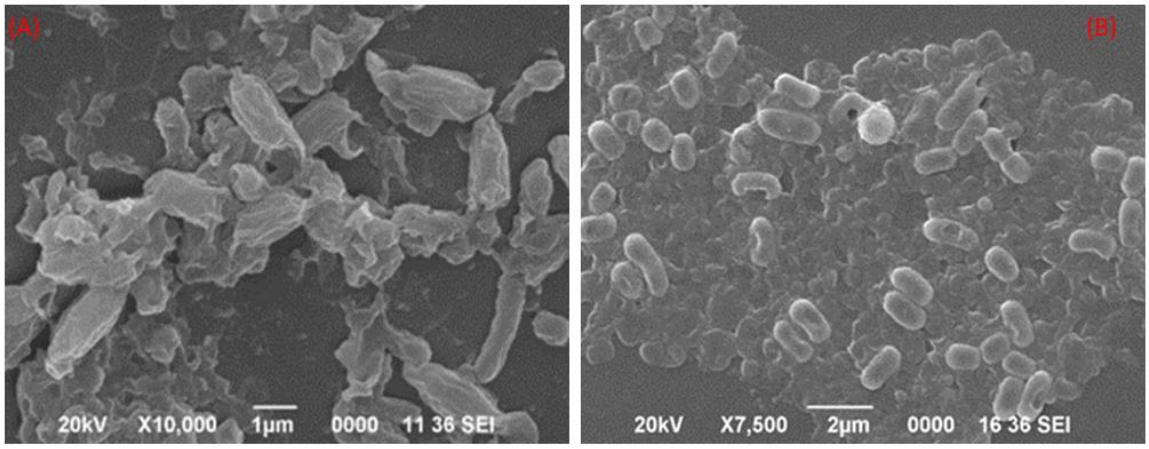

Fig. 6.10. SEM Morphological study micrographs of QM NP with *Rhizobium Sp*., magnification 10,000x (A) with *Salmonella Typhi*., magnification 7,500x (B)

Table 6.7. Plant Mineral Content (uptake of metals) under MNP treatments after harvest. Data represented as Mean ± SD.

Treatment	**Fe (mg Kg^{-1} fresh weight tissue)**	**K (mg Kg^{-1} fresh weight tissue)**	**Zn (mg Kg^{-1} fresh weight tissue)**	**Cu (mg Kg^{-1} fresh weight tissue)**	**Mn (mg Kg^{-1} fresh weight tissue)**
Control	153.9±1.3	1904.8±36.5	88.0±0.4	28.8±0.3	17.8±0.3
NPK	291.8±2.7	3788.8±67.6	92.5±0.6	25.6±0.1	24.4±0.1
VC	131.9±2.5	3567.5±114.2	128.8±0.1	18.2±0.2	51.3±0.2
FYM	186.3±1.4	3918.9±40.5	127.5±0.2	13.3±0.1	48.1±0.4
MNP25	63.1±1.4	2136.0±374.9	207.9±1.0	28.7±0.4	37.4±0.2
MNP50	89.2±2.0	2577.6±36.7	258.6±1.8	20.1±0.1	46.7±0.5
MNP100	86.0±3.3	3232.0±90.2	275.4±0.2	25.4±2.2	40.6±0.2
MNP200	96.9±0.7	3580.3±76.1	272.0±1.9	24.8±0.2	46.0±0.1
MNP250	113.7±0.3	3946.4±47.5	287.7±0.9	24.7±0.1	43.6±0.4
MNP500	117.3±0.6	3986.1±27.4	276.9±0.8	26.7±0.3	39.6±0.2
MNP1000	126.02.4	3938.4±30.5	337.1±0.4	23.9±0.9	36.1±0.2
LSD	1.6	104.5	0.8	0.6	0.2

Table 6.8. Mineral Content retention in soil after harvest under MNP treatments. Data represented as Mean ± SD.

Treatment	N (mg kg-1 dry wt. soil)	P (mg kg-1 dry wt. soil)	K (mg kg-1 dry wt. soil)	Fe (mg kg-1 dry wt. soil)	Zn (mg kg-1 dry wt. soil)	Cu (mg kg-1 dry wt. soil)	Mn (mg kg-1 dry wt. soil)
Base Soil	108.7±7.2	110.2±0.1	445.8±2.8	350.9±2.1	36.7±0.21	15.8±0.18	176.1±0.91
Control	79.4±7.2	76.1±0.1	365.2±4.5	399.3±2.1	9.6±0.04	7.6±0.07	84.1±0.68
NPK	104.1±7.6	269.8±0.3	233.5±5.9	328.9±1.6	9.6±0.26	7.4±0.22	92.3±1.85
VC	77.4±3.6	154.2±0.2	249.9±0.7	325.7±0.8	10.3±0.02	5.2±0.03	68.6±2.08
FYM	81.5±6.3	94.3±0.1	450.6±3.5	410.5±3.6	9.7±0.02	7.6±0.03	116.8±0.63
MNP25	101.6±4.5	93.9±0.1	388.6±4.6	393.9±7.4	13.0±0.04	8.8±0.43	163.9±0.80
MNP50	99.9±1.9	141.5±0.2	314.7±4.3	364.9±7.9	23.3±0.08	9.5±0.02	171.1±1.14
MNP100	101.6±4.5	91.3±0.3	357.5±6.6	426.0±3.4	22.8±0.40	10.0±0.10	179.5±1.59
MNP200	76.9±2.9	103.0±0.5	374.6±6.8	514.1±1.1	36.0±0.11	9.3±0.07	133.9±0.35
MNP250	108.7±7.2	69.3±0.1	376.4±4.7	437.0±1.5	60.4±6.16	9.0±0.07	169.6±0.81
MNP500	76.5±2.2	78.7±0.3	360.2±2.9	386.5±2.8	129.3±0.08	9.2±0.04	174.6±0.61
MNP1000	84.5±5.8	121.3±7.2	387.8±0.6	389.3±2.0	132.4±0.20	9.2±0.02	167.5±1.23
LSD	4.5	1.7	3.6	3.1	1.5	0.1	1.0

Table 6.9. Plant Mineral Content (uptake of metals) under BNP treatments after harvest. Data represented as Mean ± SD.

Treatment	Fe (mg Kg^{-1} fresh weight tissue)	K (mg Kg^{-1} fresh weight tissue)	Zn (mg Kg^{-1} fresh weight tissue)	Cu (mg Kg^{-1} fresh weight tissue)	Mn (mg Kg^{-1} fresh weight tissue)
Control	153.88±1.30	1904.80±36.46	88.00±0.35	28.82±0.34	17.81±0.26
NPK	291.77±2.71	3788.80±67.63	92.51±0.58	25.57±0.05	24.43±0.05
VC	131.92±2.53	3567.47±114.20	128.83±0.11	18.18±0.20	51.28±0.17
FYM	186.28±1.38	3918.93±40.51	127.49±0.18	13.31±0.14	48.12±0.37
BNP25	57.65±2.00	2087.73±81.83	224.83±0.77	36.91±0.17	32.31±0.40
BNP50	67.62±2.33	2646.67±235.97	247.20±0.37	47.65±0.11	28.67±0.06
BNP100	98.86±1.13	2721.33±96.72	285.36±0.70	38.99±0.27	37.43±0.13
BNP200	104.92±0.21	3154.93±141.38	298.67±0.46	141.36±1.08	37.19±0.12
BNP250	139.72±1.41	3317.60±35.09	290.72±3.48	202.59±4.34	56.50±0.45
BNP500	147.78±1.35	3290.93±40.81	310.91±0.44	50.50±0.27	53.83±0.23
BNP1000	142.72±1.00	3230.93±22.12	318.96±1.11	49.31±0.74	56.69±1.88
LSD	1.41	83.74	0.97	1.13	0.51

Table 6.10. Mineral Content retention in soil after harvest under BNP treatments. Data represented as Mean ± SD.

Treatment	N(mg kg-1 dry wt. soil)	P(mg kg-1 dry wt. soil)	K(mg kg-1 dry wt. soil)	Fe(mg kg-1 dry wt. soil)	Zn(mg kg-1 dry wt. soil)	Cu(mg kg-1 dry wt. soil)	Mn(mg kg-1 dry wt. soil)
Base Soil	108.7±7.2	110.2±0.1	445.8±2.8	350.9±2.1	36.7±0.18	15.8±0.18	176.1±0.91
Control	79.4±7.2	76.1±0.1	365.2±4.5	399.3±2.1	9.6±0.07	7.6±0.07	84.1±0.68
NPK	104.1±7.6	269.8±0.3	233.5±5.9	328.9±1.6	9.6±0.22	7.4±0.22	92.3±1.85
VC	77.4±3.6	154.2±0.2	249.9±0.7	325.7±0.8	10.3±0.03	5.2±0.03	68.6±2.08
FYM	81.5±6.3	94.3±0.1	450.6±3.5	410.5±3.6	9.7±0.03	7.6±0.03	116.8±0.68
BNP25	74.4±1.4	66.4±0.3	392.0±4.8	455.6±5.7	13.3±0.03	7.7±0.03	185.1±0.31
BNP50	108.7±7.2	66.8±0.1	376.3±1.0	469.3±1.6	23.6±0.12	9.7±0.12	175.9±0.26
BNP100	110.4±2.5	71.7±0.3	385.8±7.8	388.7±2.4	25.9±0.09	10.9±0.09	180.9±0.77
BNP200	117.1±7.2	106.0±0.2	347.7±5.3	365.3±2.1	34.3±0.09	11.6±0.09	190.7±1.03
BNP250	88.6±2.6	81.6±0.1	359.8±5.8	394.5±0.4	33.5±0.08	12.0±0.08	190.5±1.58
BNP500	117.1±7.2	74.6±0.2	356.0±3.0	386.2±3.6	97.3±0.17	19.0±0.17	190.0±1.13
BNP1000	121.3±7.2	68.3±0.1	387.8±4.0	412.7±0.6	134.4±0.04	22.7±0.04	181.5±1.05
LSD	4.9	0.2	3.7	2.2	0.3	0.1	1.0

Table 6.11. Plant Mineral Content (uptake of metals) under QMNP treatments after harvest. Data represented as Mean ± SD.

Treatments	Fe Uptake (mg Kg^{-1} fresh weight tissue)	K (mg Kg^{-1} fresh weight tissue)	Zn Uptake (mg Kg^{-1} fresh weight tissue)	Cu Uptake (mg Kg^{-1} fresh weight tissue)	Mn Uptake (mg Kg^{-1} fresh weight tissue)
Control	184.9± 54.49	1904.8±36.46	88.0± 0.35	28.8± 0.34	17.8± 0.26
NPK	291.8± 2.71	3788.8±67.63	92.5± 0.58	25.6± 0.05	24.4± 0.05
FYM	131.9± 2.53	3567.5±114.2	128.8± 0.11	18.2± 0.20	51.3± 0.17
VC	186.3± 1.38	3918.9±40.51	127.5± 0.18	13.3± 0.14	48.1± 0.37
QM10	76.5± 1.12	1903.2±105.89	135.4± 1.01	6.4± 0.08	39.9± 0.50
QM25	77.2± 1.38	2578.4±50.73	173.1± 0.57	7.3± 0.06	34.8± 0.15
QM35	92.3± 0.64	2584.8±14.06	278.1± 4.70	34.2± 0.99	31.8± 0.19
QM40	92.1± 0.87	2604.3±14.43	263.9± 0.69	36.8± 0.39	36.2± 0.17
QM45	92.0±0.53	2698.4±17.87	258.6± 4.69	37.2± 0.29	30.5± 0.08
LSD	14.88	50.988	1.85	0.32	0.21

Table 6.12. Mineral Content retention in soil after harvest under QMNP treatments. Data represented as Mean ± SD.

Treatments	Fe (mg kg^{-1} dry wt. soil)	Zn (mg kg^{-1} dry wt. soil)	Cu (mg kg^{-1} dry wt. soil)	Mn (mg kg^{-1} dry wt. soil)	Available N (mg kg^{-1} dry wt. soil)	Available P (mg kg^{-1} dry wt. soil)	Available K (mg kg^{-1} dry wt. soil)
Basic Soil	350.9± 2.06	36.7± 0.21	15.8± 0.18	176.1± 0.91	108.7±7.2	40.9±0.3	445.8±2.8
Control	399.3± 2.05	9.6± 0.04	7.5± 0.07	84.1± 0.68	79.4±7.2	110.2±0.1	365.2±4.5
NPK	328.9± 1.60	9.6± 0.26	7.4± 0.22	92.3± 1.85	104.1±7.6	76.1±0.1	233.5±5.9
FYM	325.7± 0.79	10.3± 0.02	5.2± 0.03	68.6± 2.08	77.4±3.6	269.8±0.3	249.9±0.7
VC	410.5± 3.63	9.6± 0.02	7.6± 0.03	116.8± 0.63	81.5±6.3	154.2±0.2	450.6±3.5
QM10	448.4± 1.44	20.4± 0.08	10.3± 0.10	184.1± 0.78	110.8±9.6	71.4±0.1	217.0±8.0
QM25	545.8± 2.67	20.8± 0.06	11.1± 0.02	200.8± 0.60	102.0±4.0	57.5±0.1	285.5±3.0
QM35	554.5± 2.71	24.2± 0.09	11.1± 0.04	206.3± 1.06	108.7±7.2	54.0±0.3	284.7±4.6
QM40	500.1± 2.90	23.7± 0.08	10.2± 0.03	226.5± 0.21	108.7±7.2	58.5±0.1	258.2±5.1
QM45	317.5± 3.79	22.6± 0.51	14.5± 0.12	222.7± 28.28	131.7±10.9	48.8±0.1	261.7±3.4
LSD	2.06	0.16	0.07	7.35	6.0	0.2	3.7

6.4.3.1.8. Total Bacterial and Fungal Count

Estimation of Bacterial Colonies was done immediately after harvest. Both bacterial and fungal colonies showed decreasing trend with the highest colonies in the lowest treatment group i.e., 25 mg kg^{-1} MNP, contrastingly in fungal colonies, no significant changes were noted from 25 to 100 mg kg^{-1} of MNP. Compared to FYM and Vermicompost, the different MNP treatments showed a decreasing trend except for the control and NPK treatments. Bacterial Colony Forming Unit estimation was done immediately after harvest (Fig. 6.6, 6.7). It has been observed that there is a prominent decreasing trend of bacterial colonies from 25 mg kg^{-1} to 1000 mg kg^{-1} BNP compared to control, whereas its quite clear from the graph that fungal colonies going significantly down with decreasing order from 100 mg kg^{-1} to 1000 mg kg^{-1} (Fig. 6.6.). Moreover, in QMNP treatments, both bacterial and fungal colonies showed decreasing trend from 35 mg kg^{-1} with highest colonies in the treatment group i.e., 25 mg kg^{-1} QMNP, contrastingly in fungal colonies, a significant decreasing trend was noted in all treatments compared to control (Fig. 6.7.)

6.5. Discussion

6.5.1. Bacterial Compatibility Assay

The minimum inhibitory zone discovered suggests little toxicity to soil microflora, even at levels of up to 2000 µg ml^{-1}, implying potential environmental safety of MNP, BNP and QMNP. This shows that the nanoparticles strike a good balance between antibacterial activity and environmental friendliness, making them viable candidates for agricultural uses. When a nanoparticle is added to a culture media that contains bacteria, the clear region around the

particle is known as the inhibitory zone of soil bacteria. This clean zone shows that the chemical is either killing the microorganisms there or stopping their growth. The inhibition happens as a result of the nanoparticles interfering with the growth or survival of bacterial cells, usually by the destruction of cell walls, disruption of metabolic pathways, or interference with replication[42,43]. SEM study revealed no lethal impact of 2000 µg ml^{-1} doses of MNPs, BNPs and QMNPs on *Rhizobium sp*., and *Salmonella typhi* cells, indicating their eco-friendliness for plant-soil interfaces and potential as nano-biostimulants in agriculture[44,45]. Green nanomaterials can prove to be non-toxic towards soil microflora provided the doses are less than 2000 µg ml^{-1}, necessitating comprehensive comprehension of these interactions for judicious nanotechnology application in soil management practices. This proves that the nanomaterials are eco-friendly nanomaterials that can also be applied in plant-soil interfaces without affecting the spectrum of pathogenic and non-pathogenic bacteria in the soil environment. Meanwhile, FTIR studies verifies the effective incorporation of plant extract coatings onto nanomaterial surfaces, as shown by different spectral peaks that correspond to functional groups found in the extract of plant. This supports the effective use of natural compounds to improve the stability and bioactivity of nanomaterials, paving the path for environmentally benign and sustainable nanotechnology applications.

6.5.2. Seed Germination assay and Lab scale Hydroponic farming

Monometallic Nanoparticles (MNPs) significantly improve the Germination Index (GI) and seed germination, especially at doses of 250 mg L^{-1} and 200 mg L^{-1}, demonstrating a dose-dependent effect. Excessive doses, such as 500 mg L^{-1}, resulted in a reduction in GI, probably due to cytotoxic effects that hinder seed germination[46,47]. Non-nanoscale Zn treatments hurt GI, indicating potential phytotoxicity[48]. MNPs had lower zinc absorption than non-nanoscale inorganic salts, indicating that nanoparticle and bulk forms of zinc have different bioavailability and uptake mechanisms. The recorded reductions in Relative Root Growth (RRG%), Relative Shoot Growth (RSG%), and pod yield (g/pod) in non-nanoscale inorganic salt treatments demonstrate possible negative impacts on plant growth and productivity[49–51]. Similar results were seen in Bimetallic Nanoparticle (BNP) and Quadrimetallic Nanoparticle (QNP) treatments, with varied degrees of effect on GI, seed germination, and nutrient uptake. BNP treatments, especially at 100 mg L^{-1}, resulted in lower GI, suggesting potential phytotoxic effects[46,47]. Higher concentrations of non-nanoscale Zn-Cu salt treatments resulted with substantial reductions in GI and seed germination, implying negative effects on seedling growth. Copper uptake was significantly higher in BNP-treated seeds at 500 mg L^{-1} compared to 250 mg L^{-1}, suggesting changes in metal uptake kinetics and interaction with nanoparticles.

QNP treatments had a favourable impact on GI and seed germination. Lower concentrations (e.g., 5 mg L^{-1}) produced the highest values, while higher concentrations (e.g., 45 mg L^{-1}) of non-nanoscale QNP led to decreased GI and seed germination. The reason the we observe the germination profile pass through the maxima with dosage is that the nanoparticles have become toxic after a certain dosage and has inhibitory effect to the germination of the seeds. This implies that though the synthesized nanoparticles have a positive impact on the germination, dose of application must be studied so as to avoid harmful effects to the germination. This phenomenon is also reported by Gowtham et al.[52]. The varying trends in RRG, RSG, and pod yield highlight the significance of nanoparticle the dose and composition in influencing productivity and development of plants, highlighting the need for additional research to elucidate underlying mechanisms and optimise nanoparticle-based agricultural interventions[49–51].

MNPs at doses of 200 mg L^{-1} and 250 mg L^{-1} showed good chlorophyll stability, indicating increased photosynthetic activity; lower concentrations of MNPs (50 mg L^{-1} and 100 mg L^{-1}) caused reduced chlorophyll stability, probably because to insufficient nanoparticle concentrations to trigger substantial physiological reactions. Interestingly, 500 mg L^{-1} of MNPs showed high chlorophyll stability, indicating a possible hormetic action where moderate stresses boost physiological responses[53,54]. Using 200 mg L^{-1} of non-nanoscale Zn resulted in reduced chlorophyll stability, suggesting probable phytotoxicity or disruption of chlorophyll production processes. Bimetallic Nanoparticles (BNP) treatments resulted in significantly higher chlorophyll stability (CSI) at 500 mg L^{-1}, compared to lesser doses. decreased dosages of BNPs (100 mg L^{-1} and 200 mg L^{-1}) resulted in decreased CSI, indicating insufficient nanoparticle concentrations for the required physiological response[55]. Non-nanoscale Zn-Cu treatments showed a rise in CSI at higher doses (500 mg L^{-1} and 250 mg L^{-1}), suggesting synergistic effects of zinc and copper on chlorophyll stability. Similarly, Quadrimetallic Nanoparticles (QMNPs) at treatments of 25 mg L^{-1} and 40 mg L^{-1} demonstrated significant chlorophyll stability, indicating their potential to improve the efficiency of photosynthetic activity. Conversely, lower doses of QMNPs (5 mg L^{-1} and 45 mg L^{-1}) resulted in reduced CSI, indicating insufficient concentrations to trigger physiological reactions[56].

MNPs showed poor zinc absorption at all concentrations, with the lowest uptake at 50 mg kg^{-1}, suggesting reduced bioavailability or changed uptake kinetics relative to non-nanoscale zinc salts. MNPs showed the maximum uptake at 500 mg L^{-1} and 200 mg L^{-1}, suggesting a dose-dependent trend[57,58]. Similarly, bimetallic nanoparticles (BNPs) demonstrated decreased zinc

uptake at 50 mg L^{-1}, indicating potential changes in nanoparticle interactions or bioavailability at lower doses. BNP-treated seeds showed considerably greater copper uptake at 500 mg L^{-1} and 250 mg L^{-1}, suggesting preferential uptake or improved bioavailability of copper in the presence of nanoparticles. Non-nanoscale copper showed a similar trend, with the largest increase at 500 mg L^{-1}, followed by 250 mg L^{-1}[59,60]. QMNP treatments had the maximum uptake of zinc and copper at 45 mg L^{-1}, indicating optimal concentrations for improved uptake. Iron uptake was highest at 40 mg L^{-1}, while manganese uptake peaked at 45 mg L^{-1}, suggesting concentration-dependent uptake patterns like non-nano-scale treatments[61–63].

Biochemical examination of catalase, peroxidase, and lipid peroxidation in plant cells sheds light on the oxidative stress response and antioxidant defence systems. Catalase and peroxidase activities reflect the plant's capacity to scavenge reactive oxygen species (ROS), whereas lipid peroxidation levels show the extent of oxidative damage to cellular membranes, which helps measure plant stress tolerance and physiological state[64].

Oxidative stress enzymes responded differently to MNP, BNP, and non-nanoscale Zn-Cu treatments[65,66]. MNPs induced lower catalase activity, notably at 200 mg L^{-1} followed by 500 mg L^{-1}, while non-nanoscale Zn treatments showed lower activity at 200 mg L^{-1} and 500 mg L^{-1}. Treatments with monometallic nanoparticles (MNPs) resulted in significantly decreased catalase activity than non-nanoscale zinc treatments, suggesting that nanoparticles may modulate antioxidant defence systems. MNP-treated seedlings showed decreased catalase activity, especially at concentrations of 200 mg L^{-1} and 500 mg L^{-1}, indicating a dose-dependent suppression of catalase function. Bimetallic Nanoparticles (BNPs) treatments resulted in greater catalase activity at lower doses (50 mg L^{-1}), probably due to nanoparticle-induced stress reactions. However, catalase activity reduced as BNP concentrations increased, indicating a potential hormetic response. In contrast, non-nanoscale quadrimetallic salt (QM) treatments had higher total catalase activity than QMNP treatments, regardless of application dose, implying that nanoparticles and non-nanoscale salts had different impacts on plant oxidative stress responses. Overall, oxidative damage in *Cicer arietinum* seedlings resulted from disturbances in ROS metabolism, with antioxidant enzymes playing a crucial role in mitigating ROS production[65].

Peroxidase (POD) activity varied across treatments, with MNPs showing lower activity at 100 mg L^{-1} and moderately higher at 50 mg L^{-1}. Non-nanoscale Zn treatments exhibited the highest POD activity at 250 mg L^{-1} and 500 mg L^{-1} doses, while BNP treatments showed varied

effects[66]. Non-nanoscale zinc treatments at doses of 250 mg L^{-1} and 500 mg L^{-1} showed the highest POD activity, indicating improved stress responses and antioxidant defence systems. Bimetallic Nanoparticles (BNPs) treatments had varying impacts on POD activity, with increased activity found at 50 mg L^{-1} compared to 250 mg L^{-1}, suggesting potential hormetic responses or concentration-dependent effects. Similarly, non-nanoscale Quadrimetallic Salt (QM) treatments increased POD activity, especially at higher dosages, indicating that nanoparticles and non-nanoscale salts modulate stress responses differently[50,60]. The reason we do not observe specific trends in chlorophyll stability index (CSI) and peroxidase activity (POD) in the plants because the biochemical activity of the plants shows cumulative response to various factors affected by the NPs uptake. However, we do observe reduced CSI in higher concentrations, which is a result of NP toxicity in the plants. Similarly, a lower POD in higher concentrations thus observed indicates lower inherent property of antioxidant defense (in terms of peroxidase) in Cicer arietinum seedlings. This is in line with a previous study done by Pandya et al. in 2024[67].

MNPs caused a reduction in lipid peroxidation (LPO) activity, especially at 50 mg L^{-1}, while non-nanoscale zinc salts decreased LPO activity, particularly at 50 mg L^{-1}. Conversely, non-nanoscale Zn-Cu treatments increased LPO activity at 500 mg L^{-1} and 250 mg L^{-1}[65,66]. Bimetallic Nanoparticles (BNPs) treatments increased LPO activity compared to the control, with the maximum activity found at 500 mg L^{-1}, suggesting a potential activation of oxidative stress. Similar effects were observed with non-nanoscale zinc-copper treatments, emphasising the importance of nanoparticle composition in regulating lipid peroxidation. QMNP treatments significantly reduced LPO activity, especially at lower concentrations like 5 mg L^{-1}, indicating a dose-dependent suppression of lipid peroxidation. However, higher dosages of non-nanoscale QM salt resulted in an increase in LPO activity, indicating a possible disruption of cellular redox balance[68,69].

6.5.3. Soil based study

Pot experiments require fewer financial resources than field studies, allowing for faster data collection and processing. Furthermore, pot experiments allow researchers to conduct controlled studies on certain aspects of plant growth and development, providing insights that would not be possible in a field context.

According to studies, nanoparticles can alter soil organic carbon (SOC) content, nutrient dynamics (N, P, K), and mineral availability via complicated interactions with soil

components[70,71]. Furthermore, nanoparticle applications have been connected to changes in photosynthetic processes and stomatal behaviour in plants, which may affect overall growth and productivity. Furthermore, nanoparticle-mediated alterations in soil microbial communities, such as total bacterial and fungal numbers, could have an impact on nutrient cycling and plant-microbe interactions [71].

The observed increase in soil organic carbon (SOC) after treatments with vermicompost (VC), farmyard manure (FYM), and various nanoparticle formulations demonstrate their potential to improve soil carbon sequestration. Vermicompost and FYM are known to improve soil organic matter by providing a substrate for microbial activity and encouraging carbon storage. Similarly, Monometallic Nanoparticles (MNP) treatments, particularly at a dosage of 250 mg kg^{-1}, showed considerable increases in SOC, demonstrating their potential to improve soil carbon retention[72]. Bimetallic Nanoparticles (BNP) treatments increased SOC levels, with the largest augmentation at 100 mg kg^{-1}, indicating a synergistic influence of nanoparticle composition on soil carbon dynamics. QMNP treatments resulted in significant increases in SOC, particularly at 45 mg kg^{-1}, indicating their effectiveness in enhancing soil carbon sequestration[73].

The observed variations in nitrogen (N) retention following nanoparticle treatments reflect the complex interplay between nanoparticle characteristics and soil nutrient dynamics. Monometallic Nanoparticles (MNP) treatments exhibited lower N retention at higher concentrations (200 and 500 mg kg^{-1}), possibly due to increased N leaching or immobilization processes or interactions with soil organic matter. Conversely, a higher N retention was observed at a lower concentration (50 mg kg^{-1}) of MNP, indicating a dose-dependent effect on N dynamics optimal conditions for nutrient sorption. Bimetallic Nanoparticles (BNP) treatments showed a mixed response, with lower N retention at 25 mg kg^{-1} but higher N content at other concentrations, suggesting differential effects on N availability and uptake[74–76]. Quadrimetallic Nanoparticles (QMNP) treatments resulted in overall increased available N retention in soil, highlighting their potential to enhance N availability and nutrient cycling processes. Varied nutrient retention patterns occur in response to MNP treatments[77].

MNPs play a vital role in improving plant nutrient uptake through their small size and high surface area, facilitating the absorption of vital nutrients like nitrogen, phosphorus, and potassium, consequently promoting plant growth[78]. As necessary micronutrients involved in important biochemical and physiological processes, metal atoms are crucial to plant

metabolism. Iron promotes brighter foliage and the production of metabolic energy by supporting the processes of chlorophyll synthesis, photosynthesis, and nitrogen assimilation[79]. Zinc promotes cell division and elongation by facilitating the synthesis of proteins, hormones, and enzymes[80,81]. Copper enhances the structure and durability of plants by aiding in the synthesis of lignin, photosynthetic electron transport, and stress management[82]. Manganese increases energy generation and nutrient uptake by assisting in photosynthetic water-splitting and nitrogen assimilation[83]. Treatments with Monometallic Nanoparticles (MNP) showed reduced P retention at higher concentrations of 250 mg kg^{-1}, suggesting potential P leaching or immobilization mechanisms at high nanoparticle levels. Bimetallic nanoparticle (BNP) treatments reduced soil P retention, with the highest decrease reported at 25 mg kg^{-1}, indicating a disruptive influence on P availability[84]. Higher concentrations (200 and 250 mg kg^{-1}) of BNP resulted in greater P retention, probably due to the interaction of nanoparticles with soil components that facilitate P retention. Quadri metallic Nanoparticles (QMNP) treatments enhanced available P retention in soil, showing that they have the potential to improve P availability and soil fertility[85].

Monometallic and Bimetallic Nanoparticles (BNP) treatments increased soil K retention, particularly at lower concentrations (250 mg kg^{-1}), indicating a positive impact in soil K availability. In contrast, treatments with Quadrimetallic Nanoparticles (QMNPs) resulted in a lower overall available K in soil, demonstrating that nanoparticles may interact with soil K dynamics, resulting in reduced K availability[86,87].

Monometallic Nanoparticles (MNP) treatment at 250 mg kg^{-1} increased photosynthesis and stomatal conductance, showing that nanoparticles improve plant gas exchange and carbon assimilation. MNPs may improve gas exchange, chlorophyll content, and stomatal aperture, enhancing photosynthetic efficiency and overall plant performance[88–90]. Lower concentrations of Bimetallic Nanoparticles (BNP) resulted in significantly increased photosynthesis and stomatal conductance, indicating a stimulatory influence on plant physiological activities. Similarly, Quadrimetallic Nanoparticles (QMNP) treatments evoked improved photosynthesis and stomatal conductance across multiple doses, with greater values reported at 10, 35, and 45 mg kg^{-1} [91].

The significantly enhanced peroxidase activity found in plants treated with 500 and 1000 mg kg^{-1} MNPs, regardless of growth stage, indicates that MNPs have a dose-dependent influence on peroxidase activity. Higher MNP concentrations may cause more oxidative stress in plants,

ensuing in increased peroxidase activity as part of the antioxidant defence system[92,93]. In the case of QMNP-treated plants, the maximum peroxidase activity was observed in the 40 and 45 mg kg^{-1} treatments, demonstrating a different dose-response relationship than with MNPs. This discrepancy could be attributable to variations in the physicochemical properties of nanoparticles, which result in unique interactions with plant tissues and physiological responses[94,95].

Interactions among metals and soil constituents influence nutrient retention. Interactions between metals in soil influence their uptake by plants, with competition and complexation affecting uptake patterns. Reduced Cu retention in MNP-treated soils, notably under 25 and 250 mg kg^{-1} treatments, suggests competitive interactions affecting copper stability[96–98]. Variations in metal uptake among MNP treatments may reflect differences in plant species sensitivity to metal accumulation, determined by physiological and biochemical characteristics[99–101]. Variations in soil characteristics impact nutrient retention. The concentration of MNPs significantly affects metal uptake by plants, with higher doses leading to enhanced uptake of K, Zn, and Mn (500, 1000 mg kg^{-1})[101,102]. Lower Fe uptake at 25 mg kg^{-1} and 100 mg kg^{-1} doses contrasts with higher Cu uptake at 25 mg kg^{-1} MNP application, indicating metal-specific responses[102,103]. Increased MNP concentrations enhance nutrient retention by improving availability and binding capacity in soil. Higher Fe retention in soils treated with 200 and 250 mg kg^{-1} MNP demonstrates a concentration-dependent effect[104,105]. Differences in soil texture, pH, and organic matter content may influence nutrient sorption and desorption processes across MNP treatments[106]. Nanoparticle interactions with soil components affect nutrient retention mechanisms. Enhanced Zn retention in soils treated with 250, 500, and 1000 mg kg^{-1} MNP may be attributed to favourable zinc stabilization through nanoparticle interactions[107–109]. The decrease in Fe uptake at lower BNP treatments shows a potential interference with iron uptake pathways, which could be related to competition for uptake sites or changes in soil physicochemical qualities. In contrast, the increased K absorption following BNP treatment demonstrates the stimulatory action of nanoparticles on potassium uptake systems, which may improve plant nutrient absorption efficiency[109]. The variable absorption patterns of Zn, Cu, and Mn illustrate the differential reactions of plant micronutrient uptake to BNP treatments, which are probably impacted by factors such as nanoparticle variation, soil conditions, and plant-specific nutrient demands[60,110]. The much-increased retention of Fe in MNP-treated soils, particularly at intermediate to high application rates, indicating that nanoparticles may have an affinity for iron binding sites in soil matrix,

resulting in enhanced Fe retention. Conversely, lower Zn retention in soils treated with lower MNP concentrations may be due to diminished nanoparticle-soil interactions or higher Zn leaching at lower application rates[110,111]. The divergent patterns in Cu retention, with lower levels reported in MNP-treated soils, suggest that nanoparticles may have an antagonistic influence on Cu retention mechanisms in soil. However, the fact that Mn uptake was equivalent in MNP-treated and control soils shows that nanoparticles have little effect on soil Mn dynamics[108,112]. Conversely, the constant increase in Zn, Cu, and Mn retention across BNP-treated soils suggests that soil matrices have a higher affinity for these nutrients in the presence of nanoparticles, which could be attributable to surface adsorption or complexation. In contrast, lower Zn and Cu retention in QMNP-treated soils suggests that quadrimetallic nanoparticles have a distinct effect on these nutrient retention mechanisms[86,113,114]. The enhanced Fe and Mn retention in QMNP-treated soils indicates a distinct interaction profile between quadrimetallic nanoparticles and soil nutrient pools, which could influence soil fertility and nutrient availability[110,115].

Soil microbial communities and activity levels influence nutrient dynamics. Prominent soil bacteria commonly found in *Cicer arietinum* (chickpea) include *Rhizobium spp*., Rhizobium bacteria are known for their symbiotic association with leguminous plants like chickpeas. They develop nodules on the plant roots in order to fix atmospheric nitrogen into plant available form. *Azospirillum* species are nitrogen-fixing bacteria commonly associated with the roots of grasses and cereals, including chickpeas. They can enhance the availability of nitrogen to plants. Prominent fungal colonies commonly found in the soil around Arbuscular mycorrhizal fungi (AMF), a fungi that form associations with the roots of many plant species, including chickpeas. They facilitate the nutrient uptake, especially phosphorus, from the soil. *Trichoderma* species are common soil fungi known for their properties of biocontrol. They can suppress the growth of plant pathogens and promote plant growth by enhancing nutrient uptake. While some species of *Fusarium* can be pathogenic to plants, others are beneficial and contribute to soil nutrient cycling. *Penicillium* species are ubiquitous fungi found in soil, organic matter, and decaying plant material. Some species have beneficial effects on plant growth, while others may act as plant pathogens under certain conditions. These bacteria and fungi play important roles in the soil ecosystem, contributing to nutrient cycling, disease suppression, and overall plant health in chickpea cultivation and other agricultural systems. MNP-induced alterations in microbial activity may impact nutrient cycling processes, contributing to observed variations in nutrient retention[116,117]. The observed patterns in

bacterial and fungal colonies after harvest reveal complex responses to various nanoparticle treatments. Bacterial and fungal colonies in MNP-treated soils decreased as MNP concentration increased, indicating that greater doses may have an inhibitory effect on microbial populations[118]. Fungal colonies, on the other hand, did not demonstrate any significant alterations across MNP treatments, showing that bacterial and fungal communities are not equally susceptible to MNP exposure. In BNP-treated soils, both bacterial and fungal colonies decreased with increasing BNP concentration, demonstrating BNP's general suppressive effect on microbial populations[119,120]. Similarly, in QMNP treatments, bacterial and fungal colonies decreased as QMNP concentration increased, indicating that the inhibitory effect on microbial populations is similar across treatments.

6.6. Conclusion

Nanoparticles (NPs) have sparked widespread interest in a variety of disciplines, including agriculture, due to their unique features and possible applications. Among the various types of nanoparticles, zinc (Zn), copper (Cu), iron (Fe), and manganese (Mn) monometallic, bimetallic, and quadrimetallic nanoparticles have emerged as viable agricultural options. These metallic nanoparticles provide benefits such as regulated nutrient release, increased nutrient uptake by plants, and antibacterial characteristics, which can help improve soil fertility, plant development, and agricultural productivity. Co-reduced metal nanoparticles include the simultaneous oxidation-reduction of multiple metal precursors throughout the synthesis process in plant mediated green synthesis. This process allows for the creation of alloyed nanoparticles with homogeneous compositions, which can be more stable, catalytically active, and biocompatible than nanoparticles synthesised using sequential reduction methods. Metallic nanoparticles' shape, size, aggregation, and dissolution behaviour all influence how they interact with soil, plants, and bacteria. The form and size of nanoparticles impact their uptake and transport inside plant tissues, as well as their availability to soil microbes. Smaller nanoparticles have larger surface-area to volume ratio, resulting in improved reactivity and bioavailability to plants and microorganisms. Agglomeration, or nanoparticles' inclination to form clusters or aggregates, can influence their mobility and dispersion in soil, as well as their interactions with plant roots and soil microbes. Agglomerated nanoparticles may have lower mobility and penetration into soil pores, reducing their efficiency in providing nutrients or controlling soilborne diseases. Metallic nanoparticles' dissolving behaviour in soil environments is controlled by soil pH, organic matter content, and redox conditions. Changes in soil pH can impact nanoparticle solubility and stability, influencing metal ion release and

subsequent interactions with plants and microorganisms. Metallic nanoparticles dissolve faster in acidic soils have chances of increased phytotoxicity or antibacterial properties. Nanofertilizers are designed to contain or transport critical nutrients such as nitrogen (N), phosphorus (P), potassium (K), and micronutrients in nanosized particles. These nanostructures allow for the regulated release and targeted nutrients delivery to plant roots, resulting in increased crop uptake efficiency. Nano zinc-based fertilizers and biostimulants can limit the use of conventional fertilisers by reducing nutrient losses through leaching, volatilization, and runoff, therefore minimising environmental pollution and maximising nutrient utilisation by plants. It has immense possibility to help to sustainable agriculture by lowering the environmental impact of conventional fertilisation procedures. Their precise fertiliser delivery systems reduce nutrient losses to the environment, lowering eutrophication of water bodies, soil degradation, and greenhouse gas emissions. Furthermore, the use of nanofertilizers can encourage careful fertiliser application, resulting in resource conservation, cost reductions for farmers, and long-term environmental sustainability. However, policies must be followed for recommended dose of Nanoparticles as it can accumulate in plant tissues, causing oxidative stress, DNA damage, and metabolic abnormalities. Furthermore, excessive nanoparticle application can affect soil microbial populations, disrupt nutrient cycling, and weaken soil structure, resulting in lower soil fertility and ecosystem resilience. Several factors influence the dose-dependent effects of nanoparticles on plant and soil health, including nanoparticle parameters (size, shape, surface charge), soil characteristics (pH, organic matter content, texture), plant species, and environmental circumstances. High dosages of nanoparticles can cause phytotoxicity by altering cellular processes, slowing root growth, and reducing photosynthesis. Small nanoparticles with high surface-area to volume ratios are more likely to permeate plant tissues and interact with cellular components, potentially causing negative effects even at low doses. Similarly, soil factors like pH and cation exchange capacity might affect nanoparticle stability, mobility, and bioavailability in the soil-plant system.

References

[1] Wang, Q., Zhang, P., Zhao, W., Li, Y., Jiang, Y., Rui, Y., Guo, Z., and Lynch, I. Interplay of metal-based nanoparticles with plant rhizosphere microenvironment: implications for nanosafety and nano-enabled sustainable agriculture. *Environmental Science: Nano*, 10(2):372-392, 2023.

[2] Zulfiqar, F., Navarro, M., Ashraf, M., Akram, N. A., and Munné-Bosch, S. Nanofertilizer use for sustainable agriculture: Advantages and limitations. *Plant Science*, 289:110270, 2019.

[3] Zahangeer Alam, M., Carpenter-Boggs, L., Anamul Hoque, M., and Jalal Ahammed, G. Effect of soil amendments on antioxidant activity and photosynthetic pigments in pea crops grown in arsenic contaminated soil. 20172017.

[4] Lakzian, A., Murphy, P., Turner, A., Beynon, J. L., and Giller, K. E. Rhizobium leguminosarum bv. viciae populations in soils with increasing heavy metal contamination: abundance, plasmid profiles, diversity and metal tolerance. *Soil Biology and Biochemistry*, 34(4):519-529, 2002.

[5] Bashan, Y., and de-Bashan, L. E. How the Plant Growth-Promoting Bacterium Azospirillum Promotes Plant Growth—A Critical Assessment. *Advances in Agronomy*, 108(C):77-136, 2010.

[6] Roosta, H. R., and Hamidpour, M. Effects of foliar application of some macro- and micro-nutrients on tomato plants in aquaponic and hydroponic systems. *Scientia Horticulturae*, 129(3):396-402, 2011.

[7] Majid, M., Khan, J. N., Ahmad Shah, Q. M., Masoodi, K. Z., Afroza, B., and Parvaze, S. Evaluation of hydroponic systems for the cultivation of Lettuce (Lactuca sativa L., var. Longifolia) and comparison with protected soil-based cultivation. *Agricultural Water Management*, 245:106572, 2021.

[8] Maluin, F. N., Hussein, M. Z., Wayayok, A., Nik Ibrahim, N. nor L., and Hashim, N. Chitosan nanoparticles as a sustainable alternative nutrient formulation in hydroponically grown Brassica rapa subsp. chinensis (L.) Hanelt microgreen and its adult vegetable. *Archives of Agronomy and Soil Science*, 69(12):2401-2412, 2023.

[9] Hassanein, A., Keller, E., and Lansing, S. Effect of metal nanoparticles in anaerobic

digestion production and plant uptake from effluent fertilizer. *Bioresource Technology*, 321:124455, 2021.

[10] Bauer, A. W., Kirby, W. M. M., Sherris, J. C., and Turck, M. Antibiotic susceptibility testing by a standardized single disk method. *American journal of clinical pathology*, 45(4_ts):493-496, 1966.

[11] Kim, S., and Aga, D. S. Potential ecological and human health impacts of antibiotics and antibiotic-resistant bacteria from wastewater treatment plants. *Journal of Toxicology and Environmental Health - Part B: Critical Reviews*, 10(8):559-573, 2007.

[12] Kumar, M., Tegge, W., Wangoo, N., Jain, R., and Sharma, R. K. Insights into cell penetrating peptide conjugated gold nanoparticles for internalization into bacterial cells. *Biophysical Chemistry*, 237:38-46, 2018.

[13] Devi, J., Deb, U., Barman, S., Das, S., Sundar Bhattacharya, S., Fai Tsang, Y., Lee, J. H., and Kim, K. H. Appraisal of lignocellusoic biomass degrading potential of three earthworm species using vermireactor mediated with spent mushroom substrate: Compost quality, crystallinity, and microbial community structural analysis. *Science of The Total Environment*, 716:135215, 2020.

[14] Liu, R., Zhang, H., and Lal, R. Effects of Stabilized Nanoparticles of Copper, Zinc, Manganese, and Iron Oxides in Low Concentrations on Lettuce (Lactuca sativa) Seed Germination: Nanotoxicants or Nanonutrients? *Water, Air, and Soil Pollution*, 227(1):1-14, 2016.

[15] Mahmood, J., Altaee, R., Al-Juthery, H. W. A., Al-Fadhly, J. T. M., Ali, E. A. H. M., and Al-Taee, R. A. H. G. ROLE OF SOME NANOFERTILIZERS AND ATONIKIN MAXIMIZING FOR PRODUCTION OF HYDROPONICALLY-GROWN BARLEY FODDER. *Int. J. Agricult. Stat. Sci*, 15(2):565-570, 2019. https://www.researchgate.net/publication/367519974. Accessed June 14, 2024.

[16] Yousefi, R., and Esna-Ashari, M. The effect of micro-and nanoparticles of silicon on growth and yield of strawberry in hydroponic culture. *Iranian Journal of Horticultural Science*, 51(3)2020.

[17] El-Desouky, H. S., Islam, K. R., Bergefurd, B., Gao, G., Harker, T., Abd-El-Dayem,

H., Ismail, F., Mady, M., and Zewail, R. M. Y. Nano iron fertilization significantly increases tomato yield by increasing plants' vegetable growth and photosynthetic efficiency. *Journal of Plant Nutrition*, 44(11):1649-1663, 2021.

[18] Shahid, S., Imtiaz, H., Rashid, J., Xu, M., Vithanage, M., and Ahmad, M. Uptake, translocation, and nutrient efficiency of nano-bonechar as a plant growth regulator in hydroponics and soil systems. *Environmental Research*, 251:118695, 2024.

[19] Nazarideljou, M. J., Rahmani, S., Kalanaky, S., Hojati, M., and Nazaran, M. H. Nanochelating-based fertilizers: Innovations for yield enhancement in hydroponic cultivation. *Scientia Horticulturae*, 326:112776, 2024.

[20] Anderson, J. M., and Boardman, N. K. Fractionation of the photochemical systems of photosynthesis I. Chlorophyll contents and photochemical activities of particles isolated from spinach chloroplasts. *Biochimica et Biophysica Acta (BBA) - Biophysics including Photosynthesis*, 112(3):403-421, 1966.

[21] Sairam, R. K., Deshmukh, P. S., and Shukla, D. S. Tolerance of Drought and Temperature Stress in Relation to Increased Antioxidant Enzyme Activity in Wheat. *Journal of Agronomy and Crop Science*, 178(3):171-178, 1997.

[22] Ma, J. F., Goto, S., Tamai, K., and Ichii, M. Role of Root Hairs and Lateral Roots in Silicon Uptake by Rice. *Plant Physiology*, 127(4):1773-1780, 2001.

[23] Aebi, H. Oxygen Radicals in Biological Systems - Catalase in Vitro. *Methods in Enzymology*, 105(1947):121-126, 1984. http://www.sciencedirect.com/science/article/pii/S0076687984050163. Accessed October 18, 2023.

[24] Pütter, J. Peroxidases. *Methods of Enzymatic Analysis*, January 1974:685-690, 1974.

[25] Halliwell, B., and Chirico, S. Lipid peroxidation: its mechanism, measurement, and significance. *The American Journal of Clinical Nutrition*, 57(5):715S-725S, 1993.

[26] Goswami, L., Patel, A. K. uma., Dutta, G., Bhattacharyya, P., Gogoi, N., and Bhattacharya, S. S. unda. Hazard remediation and recycling of tea industry and paper mill bottom ash through vermiconversion. *Chemosphere*, 92(6):708-713, 2013.

[27] Das, P., Barua, S., Sarkar, S., Chatterjee, S. K., Mukherjee, S., Goswami, L., Das, S., Bhattacharya, S., Karak, N., and Bhattacharya, S. S. Mechanism of toxicity and

transformation of silver nanoparticles: Inclusive assessment in earthworm-microbe-soil-plant system. *Geoderma*, 314:73-84, 2018.

[28] Goldin, A. Reassessing the use of loss-on-ignition for estimating organic matter content in noncalcareous soils. *Communications in Soil Science and Plant Analysis*, 18(10):1111-1116, 1987.

[29] Matejovic, I. Total nitrogen in plant material determinated by means of dry combustion: A possible alternative to determination by Kjeldahl digestion. *Communications in Soil Science and Plant Analysis*, 26(13-14):2217-2229, 1995.

[30] Bray, R. ., and Kurtz, L. . Determination of total, organic, and available forms of phosphorus in soils. *Soil science*, 59(1):39-46, 1945.

[31] Fixen, P. E., and Grove, J. H. Testing soils for phosphorus. *Soil testing and plant analysis*, 3:141-180, 1990.

[32] Pettigrew, W. T. Potassium influences on yield and quality production for maize, wheat, soybean and cotton. *Physiologia Plantarum*, 133(4):670-681, 2008.

[33] Yanagi, T., Okamoto, K., and Takita, S. Effect of blue and red light intensity on photo synthetic rate of strawberry leaves. *Acta Horticulturae*, 440:371-376, 1996.

[34] Amthor, J. S. Direct effect of elevated CO2 on nocturnal in situ leaf respiration in nine temperate deciduous tree species is small. *Tree Physiology*, 20(2):139-144, 2000.

[35] Kingston, H. M., and Jassie, L. B. Microwave Energy for Acid Decomposition at Elevated Temperatures and Pressures Using Biological and Botanical Samples. *Analytical Chemistry*, 58(12):2534-2541, 1986.

[36] Petterson, D. S., Sipsas, S., and Mackintosh, J. B. *The Chemical Composition and Nutritive Value of Australian Pulses.* 2nd ed. (Petterson DS, Sipsas S, Mackintosh JB, eds.). Kingston, Australia: Grains Research and Development Corporation; 1997.

[37] Sah, R. N., and Miller, R. O. Spontaneous Reaction for Acid Dissolution of Biological Tissues in Closed Vessels. *Analytical Chemistry*, 64(2):230-233, 1992.

[38] Pramer, D. E., and Schmidt, E. L. *Experimental Soil Microbiology*. Minneapolis, USA: Burges publishing company; 1964.

[39] Bhattacharya, S. S., Barman, S., Ghosh, R., Duary, R. K., Goswami, L., and Mandal,

N. C. Phosphate solubilizing ability of Emericella nidulans strain V1 isolated from vermicompost. *Indian Journal of Experimental Biology*, 51:840-848, 2013.

[40] García-López, J. I., Niño-Medina, G., Olivares-Sáenz, E., Lira-Saldivar, R. H., Barriga-Castro, E. D., Vázquez-Alvarado, R., Rodríguez-Salinas, P. A., and Zavala-García, F. Foliar Application of Zinc Oxide Nanoparticles and Zinc Sulfate Boosts the Content of Bioactive Compounds in Habanero Peppers. *Plants 2019, Vol. 8, Page 254*, 8(8):254, 2019.

[41] Venkatachalam, P., Jayaraj, M., Manikandan, R., Geetha, N., Rene, E. R., Sharma, N. C., and Sahi, S. V. Zinc oxide nanoparticles (ZnONPs) alleviate heavy metal-induced toxicity in Leucaena leucocephala seedlings: A physiochemical analysis. *Plant Physiology and Biochemistry*, 110:59-69, 2017.

[42] C Gould, B. J., and Bowie, J. H. The Determination of Bacterial Sensitivity to Antibiotics. *Edinburgh Medical Journal*, 59(4):178, 1952.

[43] Gogoi, N., Babu, P. J., Mahanta, C., and Bora, U. Green synthesis and characterization of silver nanoparticles using alcoholic flower extract of Nyctanthes arbortristis and in vitro investigation of their antibacterial and cytotoxic activities. *Materials Science and Engineering: C*, 46:463-469, 2015.

[44] Ahmed, T., Noman, M., Shahid, M., Niazi, M. B. K., Hussain, S., Manzoor, N., Wang, X., and Li, B. Green synthesis of silver nanoparticles transformed synthetic textile dye into less toxic intermediate molecules through LC-MS analysis and treated the actual wastewater. *Environmental Research*, 191:110142, 2020.

[45] Saleem, S., and Khan, M. S. Phyto-interactive impact of green synthesized iron oxide nanoparticles and Rhizobium pusense on morpho-physiological and yield components of greengram. *Plant Physiology and Biochemistry*, 194:146-160, 2023.

[46] Nouairi, I., Jalali, K., Essid, S., Zribi, K., and Mhadhbi, H. Alleviation of cadmium-induced genotoxicity and cytotoxicity by calcium chloride in faba bean (Vicia faba L. var. minor) roots. *Physiology and Molecular Biology of Plants*, 25(4):921-931, 2019.

[47] Guha, T., Ravikumar, K. V. G., Mukherjee, A., Mukherjee, A., and Kundu, R. Nanopriming with zero valent iron (nZVI) enhances germination and growth in aromatic rice cultivar (Oryza sativa cv. Gobindabhog L.). *Plant Physiology and*

Biochemistry, 127:403-413, 2018.

[48] Essa, H. L., Abdelfattah, M. S., Marzouk, A. S., Shedeed, Z., Guirguis, H. A., and El-Sayedi, M. M. H. Biogenic copper nanoparticles from Avicennia marina leaves: Impact on seed germination, detoxification enzymes, chlorophyll content and uptake by wheat seedlings. *PLOS ONE*, 16(4):e0249764, 2021.

[49] Yadav, A., Babu, S., Krishnan, P., Kaur, B., Bana, R. S., Chakraborty, D., Kumar, V., Joshi, B., and Lal, S. K. Zinc oxide and ferric oxide nanoparticles combination increase plant growth, yield, and quality of soybean under semiarid region. *Chemosphere*, 352:141432, 2024.

[50] Mohamadzadeh, M., Janmohammadi, M., Abbasi, A., Sabaghnia, N., and Ion, V. Physiochemical response of Cicer arietinum to zinc-containing mesoporous silica nanoparticles under water stress. *BioTechnologia*, 104(3):263, 2023.

[51] Hussain, M., Farooq, S., Hasan, W., Ul-Allah, S., Tanveer, M., Farooq, M., and Nawaz, A. Drought stress in sunflower: Physiological effects and its management through breeding and agronomic alternatives. *Agricultural Water Management*, 201:152-166, 2018.

[52] Gowtham, H. G., Shilpa, N., Singh, S. B., Aiyaz, M., Abhilash, M. R., Nataraj, K., Amruthesh, K. N., Ansari, M. A., Alomary, M. N., and Murali, M. Toxicological effects of nanoparticles in plants: Mechanisms involved at morphological, physiological, biochemical and molecular levels. *Plant Physiology and Biochemistry*, 210:108604, 2024.

[53] Rai, P. K., Song, H., and Kim, K. H. Nanoparticles modulate heavy-metal and arsenic stress in food crops: Hormesis for food security/safety and public health. *Science of The Total Environment*, 902:166064, 2023.

[54] Ghorbanpour, M., and Askary, F. Comparative study on the morpho-physiological responses and alkaloids content in Eschscholzia californica cham to foliar applied α-Fe2O3 NPs and ferric ions. *Industrial Crops and Products*, 214:118484, 2024.

[55] Bhattacharya, S., Gupta, S., and Saha, J. Nanoparticles regulate redox metabolism in plants during abiotic stress within hormetic boundaries. *Functional Plant Biology*, 50(11):850-869, 2023.

[56] Fatehi, S. F., Oraei, M., Gohari, G., Akbari, A., and Faramarzi, A. Proline-Functionalized Graphene Oxide Nanoparticles (GO–Pro NPs) Mitigate Salt-Induced Adverse Effects on Morpho-Physiological Traits and Essential Oils Constituents in Moldavian Balm (Dracocephalum moldavica L.). *Journal of Plant Growth Regulation*, 41(7):2818-2832, 2021.

[57] Burman, U., Saini, M., and Kumar, P. Effect of zinc oxide nanoparticles on growth and antioxidant system of chickpea seedlings. *Toxicological & Environmental Chemistry*, 95(4):605-612, 2013.

[58] Ullah, A., Farooq, M., Rehman, A., Hussain, M., and Siddique, K. H. M. Zinc nutrition in chickpea (Cicer arietinum): a review. *Crop and Pasture Science*, 71(3):199-218, 2020.

[59] Tiwari, V., Bambharoliya, K. S., Bhatt, M. D., Nath, M., Arora, S., Dobriyal, A. K., and Bhatt, D. Application of green synthesized copper oxide nanoparticles for effective mitigation of Fusarium wilt disease in roots of Cicer arietinum. *Physiological and Molecular Plant Pathology*, 131:102244, 2024.

[60] Tului, V., Janmohammadi, M., Abbasi, A., Vahdati-Khajeh, S., and Nouraein, M. Influence of iron, zinc and bimetallic zn-fe nanoparticles on growth and biochemical characteristics in chickpea (Cicer arietinum) cultivars. *Agriculture and Forestry*, 67(2):179-193, 2021.

[61] Zhang, C., Liu, J., Zhao, T., Gomez, A., Li, C., Yu, C., Li, H., Lin, J., Yang, Y., Liu, B., and Lin, C. A drought-inducible transcription factor delays reproductive timing in rice. *Plant Physiology*, 171(1):334-343, 2016.

[62] Rana, K., Kumari, M., Mishra, A., and Pudake, R. N. Engineered Nanoparticles for Increasing Micronutrient Use Efficiency. *Nanoscience for Sustainable Agriculture*, September 2019:25-49, 2019.

[63] Priyanka, N., Geetha, N., Ghorbanpour, M., and Venkatachalam, P. Role of Engineered Zinc and Copper Oxide Nanoparticles in Promoting Plant Growth and Yield: Present Status and Future Prospects. *Advances in Phytonanotechnology: From Synthesis to Application*, January 2019:183-201, 2019.

[64] Taiz, L., Zeiger, E., Møller, I. M., and Murphy, A. Plant physiology and Development.

20152015.

[65] Rai-Kalal, P., and Jajoo, A. Priming with zinc oxide nanoparticles improve germination and photosynthetic performance in wheat. *Plant Physiology and Biochemistry*, 160:341-351, 2021.

[66] Rai-Kalal, P., Tomar, R. S., and Jajoo, A. H2O2 signaling regulates seed germination in ZnO nanoprimed wheat (Triticum aestivum L.) seeds for improving plant performance under drought stress. *Environmental and Experimental Botany*, 189:104561, 2021.

[67] Pandya, P., Kumar, S., Patil, G., Mankad, M., and Shah, Z. Impact of ZnO nanopriming on physiological and biochemical traits of wheat (Triticum aestivum L.) seedling. *CABI Agriculture and Bioscience*, 5(1):1-15, 2024.

[68] Basumatary, A., Ahmed, S., and Das, K. N. Soil test based fertilizer prescriptions under integrated plant nutrient supply for rice-rice cropping sequence in Inceptisols of Assam. *Journal of the Indian Society of Soil Science*, 63(2):186-190, 2015.

[69] Ashok, A., Kumar, A., and Tarlochan, F. Preparation of nanoparticles via cellulose-assisted combustion synthesis. *International Journal of Self-Propagating High-Temperature Synthesis*, 27:141-153, 2018.

[70] Das, P., Sarmah, K., Hussain, N., Pratihar, S., Das, S., Bhattacharyya, P., Patil, S. A., Kim, H. S., Khazi, M. I. A., and Bhattacharya, S. S. Novel synthesis of an iron oxalate capped iron oxide nanomaterial: a unique soil conditioner and slow release eco-friendly source of iron sustenance in plants. *RSC Advances*, 6(105):103012-103025, 2016.

[71] Das, P., Gogoi, N., Sarkar, S., Patil, S. A., Hussain, N., Barman, S., Pratihar, S., and Bhattacharya, S. S. Nano-based soil conditioners eradicate micronutrient deficiency: soil physicochemical properties and plant molecular responses. *Environmental Science: Nano*, 8(10):2824-2843, 2021.

[72] Jośko, I. Copper and zinc fractionation in soils treated with CuO and ZnO nanoparticles: The effect of soil type and moisture content. *Science of The Total Environment*, 653:822-832, 2019.

[73] Sun, J., Zhou, S., Hou, P., Yang, Y., Weng, J., Li, X., and Li, M. Synthesis and

characterization of biocompatible Fe3O4 nanoparticles. *Journal of Biomedical Materials Research Part A*, 80A(2):333-341, 2007.

[74] Jones, O. R., Stewart, B. A., and Unger, P. W. Management of Dry-Farmed Southern Great Plains Soils for Sustained Productivity. *Soil Organic Matter in Temperate Agroecosystems*, August 2019:387-401, 2019.

[75] Moreau, D., Bardgett, R. D., Finlay, R. D., Jones, D. L., and Philippot, L. A plant perspective on nitrogen cycling in the rhizosphere. *Functional Ecology*, 33(4):540-552, 2019.

[76] Beig, B., Niazi, M. B. K., Jahan, Z., Haider, G., Zia, M., Shah, G. A., Iqbal, Z., and Hayat, A. Development and testing of zinc sulfate and zinc oxide nanoparticle-coated urea fertilizer to improve N and Zn use efficiency. *Frontiers in Plant Science*, 13:1058219, 2023.

[77] Shirvani, M., and Ghalandari, Y. Effects of zinc oxide nanoparticles on carbon mineralization kinetics and microbial attributes in plant residue-amended soils. *Environmental Nanotechnology, Monitoring & Management*, 21:100939, 2024.

[78] Yadav, A. N. Plant Microbiomes for Sustainable Agriculture: Current Research and Future Challenges. 2020:475-482, 2020.

[79] Li, M., Zhang, P., Adeel, M., Guo, Z., Chetwynd, A. J., Ma, C., Bai, T., Hao, Y., and Rui, Y. Physiological impacts of zero valent iron, Fe3O4 and Fe2O3 nanoparticles in rice plants and their potential as Fe fertilizers. *Environmental Pollution*, 269:116134, 2021.

[80] Azmat, A., Tanveer, Y., Yasmin, H., Hassan, M. N., Shahzad, A., Reddy, M., and Ahmad, A. Coactive role of zinc oxide nanoparticles and plant growth promoting rhizobacteria for mitigation of synchronized effects of heat and drought stress in wheat plants. *Chemosphere*, 297:133982, 2022.

[81] Sun, L., Wang, Y., Wang, R., Wang, R., Zhang, P., Ju, Q., and Xu, J. Physiological, transcriptomic, and metabolomic analyses reveal zinc oxide nanoparticles modulate plant growth in tomato. *Environmental Science: Nano*, 7(11):3587-3604, 2020.

[82] Lopez-Lima, D., Mtz-Enriquez, A. I., Carrión, G., Basurto-Cereceda, S., and Pariona, N. The bifunctional role of copper nanoparticles in tomato: Effective treatment for

Fusarium wilt and plant growth promoter. *Scientia Horticulturae*, 277:109810, 2021.

[83] de França Bettencourt, G. M., Degenhardt, J., Zevallos Torres, L. A., de Andrade Tanobe, V. O., and Soccol, C. R. Green biosynthesis of single and bimetallic nanoparticles of iron and manganese using bacterial auxin complex to act as plant bio-fertilizer. *Biocatalysis and Agricultural Biotechnology*, 30:101822, 2020.

[84] Taghipour, M., and Jalali, M. Effect of nanoparticles on kinetics release and fractionation of phosphorus. *Journal of Hazardous Materials*, 283:359-370, 2015.

[85] Moharami, S., and Jalali, M. Effect of time on the sorption and distribution of phosphorus in treated soil with minerals and nanoparticles. *Environmental Earth Sciences*, 73(12):8599-8608, 2015.

[86] Dimkpa, C. O., Singh, U., Bindraban, P. S., Adisa, I. O., Elmer, W. H., Gardea-Torresdey, J. L., and White, J. C. Addition-omission of zinc, copper, and boron nano and bulk oxide particles demonstrate element and size -specific response of soybean to micronutrients exposure. *Science of The Total Environment*, 665:606-616, 2019.

[87] Zörb, C., Senbayram, M., and Peiter, E. Potassium in agriculture – Status and perspectives. *Journal of Plant Physiology*, 171(9):656-669, 2014.

[88] Li, Y., Kong, T., and Shen, S. Artificial Photosynthesis with Polymeric Carbon Nitride: When Meeting Metal Nanoparticles, Single Atoms, and Molecular Complexes. *Small*, 15(32):1900772, 2019.

[89] Wang, J., Liu, C., Hussain, I., Li, C., Li, J., Sun, X., Shen, J., Han, W., and Wang, L. Iron-copper bimetallic nanoparticles supported on hollow mesoporous silica spheres: The effect of Fe/Cu ratio on heterogeneous Fenton degradation of a dye. *RSC Advances*, 6(59):54623-54635, 2016.

[90] Wang, X., Yin, R., Zeng, L., and Zhu, M. A review of graphene-based nanomaterials for removal of antibiotics from aqueous environments. *Environmental Pollution*, 253:100-110, 2019.

[91] Pedruzzi, D. P., Araujo, L. O., Falco, W. F., Machado, G., Casagrande, G. A., Colbeck, I., Lawson, T., Oliveira, S. L., and Caires, A. R. L. ZnO nanoparticles impact on the photosynthetic activity of Vicia faba: Effect of particle size and concentration. *NanoImpact*, 19:100246, 2020.

[92] Gupta, N., Jain, S. K., Tomar, B. S., Anand, A., Singh, J., Sagar, V., Kumar, R., Singh, V., Chaubey, T., Abd-Elsalam, K. A., and Singh, A. K. Impact of Foliar Application of ZnO and Fe3O4 Nanoparticles on Seed Yield and Physio-Biochemical Parameters of Cucumber (Cucumis sativus L.) Seed under Open Field and Protected Environment vis a vis during Seed Germination. *Plants*, 11(23):3211, 2022.

[93] Kumar, A., Singh, I. K., Mishra, R., Singh, A., Ramawat, N., and Singh, A. The Role of Zinc Oxide Nanoparticles in Plants: A Critical Appraisal. *Nanotechnology in the Life Sciences*, 2021:249-267, 2021.

[94] Rizwan, M., Ali, S., Ali, B., Adrees, M., Arshad, M., Hussain, A., Zia ur Rehman, M., and Waris, A. A. Zinc and iron oxide nanoparticles improved the plant growth and reduced the oxidative stress and cadmium concentration in wheat. *Chemosphere*, 214:269-277, 2019.

[95] Perfileva, A. I., Lipchanskaya, T. V., Kharasova, A. R., Nozhkina, O. A., Putilina, T. Y., Sidorov, A. V., Kon'kova, T. V., and Sukhov, B. G. Physiological and Biochemical Parameters of In Vitro Potato Plants Cultured on Media with Manganese-Hydroxide and Copper-Oxide Nanocomposites in an Arabinogalactan Matrix. *Nanobiotechnology Reports*, 18(3):467-474, 2023.

[96] Shi, J., Wu, Q., Zheng, C., and Yang, J. The interaction between particulate organic matter and copper, zinc in paddy soil. *Environmental Pollution*, 243:1394-1402, 2018.

[97] Lair, G. J., Gerzabek, M. H., and Haberhauer, G. Retention of copper, cadmium and zinc in soil and its textural fractions influenced by long-term field management. *European Journal of Soil Science*, 58(5):1145-1154, 2007.

[98] Mouta, E. R., Soares, M. R., and Casagrande, J. C. Copper adsorption as a function of solution parameters of variable charge soils. *Journal of the Brazilian Chemical Society*, 19(5):996-1009, 2008.

[99] JUNAID, M., ADNAN, M., KHAN, N., KHAN, N., RAHMAN, M.-U.-, and ALI, N. PLANT GROWTH, BIOCHEMICAL CHARACTERISTICS AND HEAVY METALS CONTENTS OF MEDICAGO SATIVA L., BRASSICA JUNCEA (L.) CZERN. AND CICER ARIETINUM L. *FUUAST Journal of Biology*, 3(2):95-103, 2013. https://fuuastjb.org/index.php/fuuastjb/article/view/246. Accessed June 14, 2024.

[100] Imtiaz, M., Tu, S., Xie, Z., Han, D., Ashraf, M., and Rizwan, M. S. Growth, V uptake, and antioxidant enzymes responses of chickpea (Cicer arietinum L.) genotypes under vanadium stress. *Plant and Soil*, 390(1-2):17-27, 2015.

[101] Wani, P. A., Khan, M. S., and Zaidi, A. Impact of heavy metal toxicity on plant growth, symbiosis, seed yield and nitrogen and metal uptake in chickpea. *Australian Journal of Experimental Agriculture*, 47(6):712-720, 2007.

[102] Narendrula-Kotha, R., Theriault, G., Mehes-Smith, M., Kalubi, K., and Nkongolo, K. Metal Toxicity and Resistance in Plants and Microorganisms in Terrestrial Ecosystems. *Reviews of Environmental Contamination and Toxicology*, 249:1-27, 2019.

[103] Das, R. K., Gogoi, N., Babu, P. J., Sharma, P., Mahanta, C., and Bora, U. The Synthesis of Gold Nanoparticles Using <i>Amaranthus spinosus</i> Leaf Extract and Study of Their Optical Properties. *Advances in Materials Physics and Chemistry*, 02(04):275-281, 2012.

[104] Schrick, B., Hydutsky, B. W., Blough, J. L., and Mallouk, T. E. Delivery vehicles for zerovalent metal nanoparticles in soil and groundwater. *Chemistry of Materials*, 16(11):2187-2193, 2004.

[105] Cornelis, G., Thomas, C. D., McLaughlin, M. J., Kirby, J. K., Beak, D. G., and Chittleborough, D. Retention and Dissolution of Engineered Silver Nanoparticles in Natural Soils. *Soil Science Society of America Journal*, 76(3):891-902, 2012.

[106] Jagathesan, G., and Rajiv, P. Biosynthesis and characterization of iron oxide nanoparticles using Eichhornia crassipes leaf extract and assessing their antibacterial activity. *Biocatalysis and Agricultural Biotechnology*, 13:90-94, 2018.

[107] Xu, M., Wang, Y., Mu, Z., Li, S., and Li, H. Dissolution of copper oxide nanoparticles is controlled by soil solution pH, dissolved organic matter, and particle specific surface area. *Science of The Total Environment*, 772:145477, 2021.

[108] Gao, C., El-Sawah, A. M., Ismail Ali, D. F., Hamoud, Y. A., Shaghaleh, H., and Sheteiwy, M. S. The Integration of Bio and Organic Fertilizers Improve Plant Growth, Grain Yield, Quality and Metabolism of Hybrid Maize (Zea mays L.). *Agronomy 2020, Vol. 10, Page 319*, 10(3):319, 2020.

[109] Denisse, V. G. J., Roberto, S. C. C., Hermes, P. H., Patricio, T. G. A., Andrea, P. M., and Fabián, F. L. Influence of nanoparticles on the physical, chemical, and biological properties of soils. *Nanomaterials for Soil Remediation*, January 2021:151-182, 2021.

[110] Faraz, A., Faizan, M., Sami, F., Siddiqui, H., Pichtel, J., and Hayat, S. Nanoparticles: biosynthesis, translocation and role in plant metabolism. *IET Nanobiotechnology*, 13(4):345-352, 2019.

[111] Ulhassan, Z., Khan, A. R., Hamid, Y., Azhar, W., Hussain, S., Sheteiwy, M. S., Salam, A., Hakeem, K. R., and Zhou, W. Interaction of nanoparticles with soil–plant system and their usage in remediation strategies. *Metals and Metalloids in Soil-Plant-Water Systems: Phytophysiology and Remediation Techniques*, January 2022:287-308, 2022.

[112] Dlugaszewska, J., and Dobrucka, R. Effectiveness of biosynthesized trimetallic Au/Pt/Ag nanoparticles on planktonic and biofilm Enterococcus faecalis and Enterococcus faecium forms. *Journal of Cluster Science*, 30:1091-1101, 2019.

[113] Sturikova, H., Krystofova, O., Huska, D., and Adam, V. Zinc, zinc nanoparticles and plants. *Journal of Hazardous Materials*, 349:101-110, 2018.

[114] Rani, S., Kumari, N., and Sharma, V. Uptake, translocation, transformation and physiological effects of nanoparticles in plants. *Archives of Agronomy and Soil Science*, July 20232023.

[115] Arif, N., Yadav, V., Singh, S., Tripathi, D. K., Dubey, N. K., Chauhan, D. K., and Giorgetti, L. Interaction of Copper Oxide Nanoparticles With Plants: Uptake, Accumulation, and Toxicity. *Nanomaterials in Plants, Algae, and Microorganisms*, 1:297-310, 2018.

[116] Vishwakarma, A., Kumar, A., Samte, M., Parbo, D., and Krishna, M. Remnant Flowering Trees as Avifaunal Refuge in the Fringe Areas of Pakke Tiger Reserve, Arunachal Pradesh, India. *Proceedings of the Zoological Society*, 74(3):249-261, 2021.

[117] Boddupalli, A., Tiwari, R., Sharma, A., Singh, S., Prasanna, R., and Nain, L. Elucidating the interactions and phytotoxicity of zinc oxide nanoparticles with agriculturally beneficial bacteria and selected crop plants. *Folia Microbiologica*, 62(3):253-262, 2017.

[118] Kaur, H., Kalia, A., Sandhu, J. S., Dheri, G. S., Kaur, G., and Pathania, S. Interaction

of TiO2 nanoparticles with soil: Effect on microbiological and chemical traits. *Chemosphere*, 301:134629, 2022.

[119] Godoy-Gallardo, M., Eckhard, U., Delgado, L. M., de Roo Puente, Y. J. D., Hoyos-Nogués, M., Gil, F. J., and Perez, R. A. Antibacterial approaches in tissue engineering using metal ions and nanoparticles: From mechanisms to applications. *Bioactive Materials*, 6(12):4470-4490, 2021.

[120] Shah, G. M., Ali, H., Ahmad, I., Kamran, M., Hammad, M., Shah, G. A., Bakhat, H. F., Waqar, A., Guo, J., Dong, R., and Rashid, M. I. Nano agrochemical zinc oxide influences microbial activity, carbon, and nitrogen cycling of applied manures in the soil-plant system. *Environmental Pollution*, 293:118559, 2022.